

Detecting materials for HEP applications: future of inorganic scintillators

Mikhail Korzhik

INP BSU, Minsk, Belarus

NRC “Kurchatov Institute”, Moscow, Russian Federation

What is the role of the ionizing radiation detectors in the progress of this century?

Three lasting tasks:

- **Future compacting, storage and extraction of the energy;**
Chemical-Nuclear-?
- **Signature for the industrial progress;**
Ruler-Microscope-?
- **A frontier between living and non-living .**
Downfall-Ordering-Chaos-?

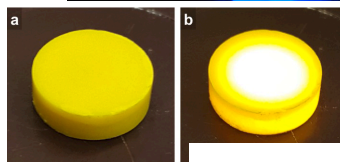
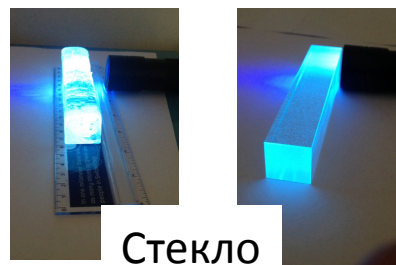
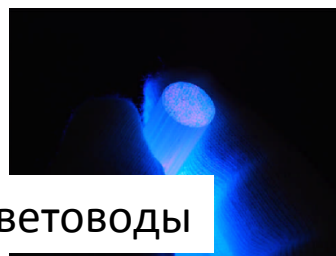
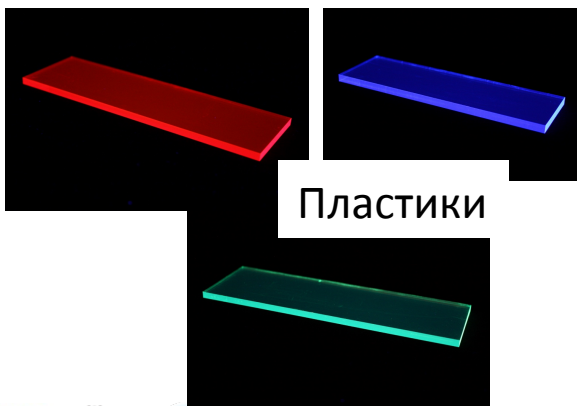
Outline

- **Scintillation & Scintillators;**
- **Modern trend in development;**
- **Engineering of the properties;**
- **Toward fast timing;**
- **On the radiation tolerance of the materials;**
- **Toward the photo-sensor free detecting technologies;**
- **Implementations;**

What is a scintillation ?

СЦИНТИЛЛЯЦИЯ- люминесценция, возникающая в прозрачной среде при взаимодействии с ионизирующим излучением.

- В случае фотонов и частиц, взаимодействующих с ядрами среды, необходимым условием возникновения сцинтилляций является прохождение через среду.
- В случае заряженных частиц условием возникновения сцинтилляций является прохождение через среду либо вблизи среды.
- Сцинтилляция-слабый оптический сигнал, поэтому требуются чувствительные фотоприемники либо фотоприемники с значительным усилением.



Кристаллы

Жидкости
и
газы




Lead tungstate crystalline material is the most widely applied scintillator at experiments at colliders

density: $8,28\text{gcm}^3$; decay time constant-10 ns; Light Yield 200 ph/MeV

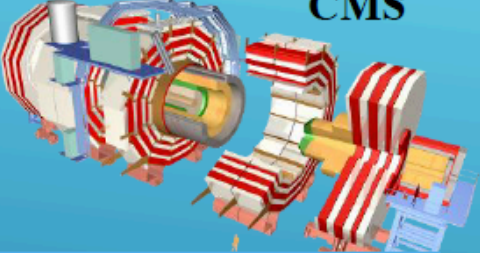
CERN-LHC Program

ALICE :17920 crystals



Alice

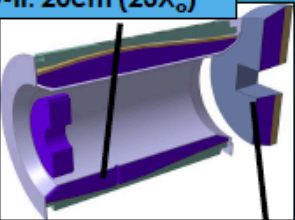
CMS



75848 crystals = 100 tons

PANDA at FAIR (GSI)

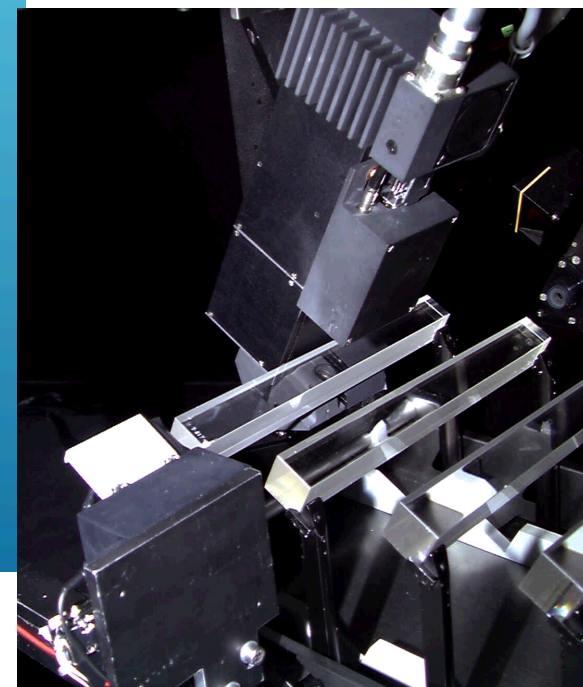
PWO-II: 20cm ($23X_0$)



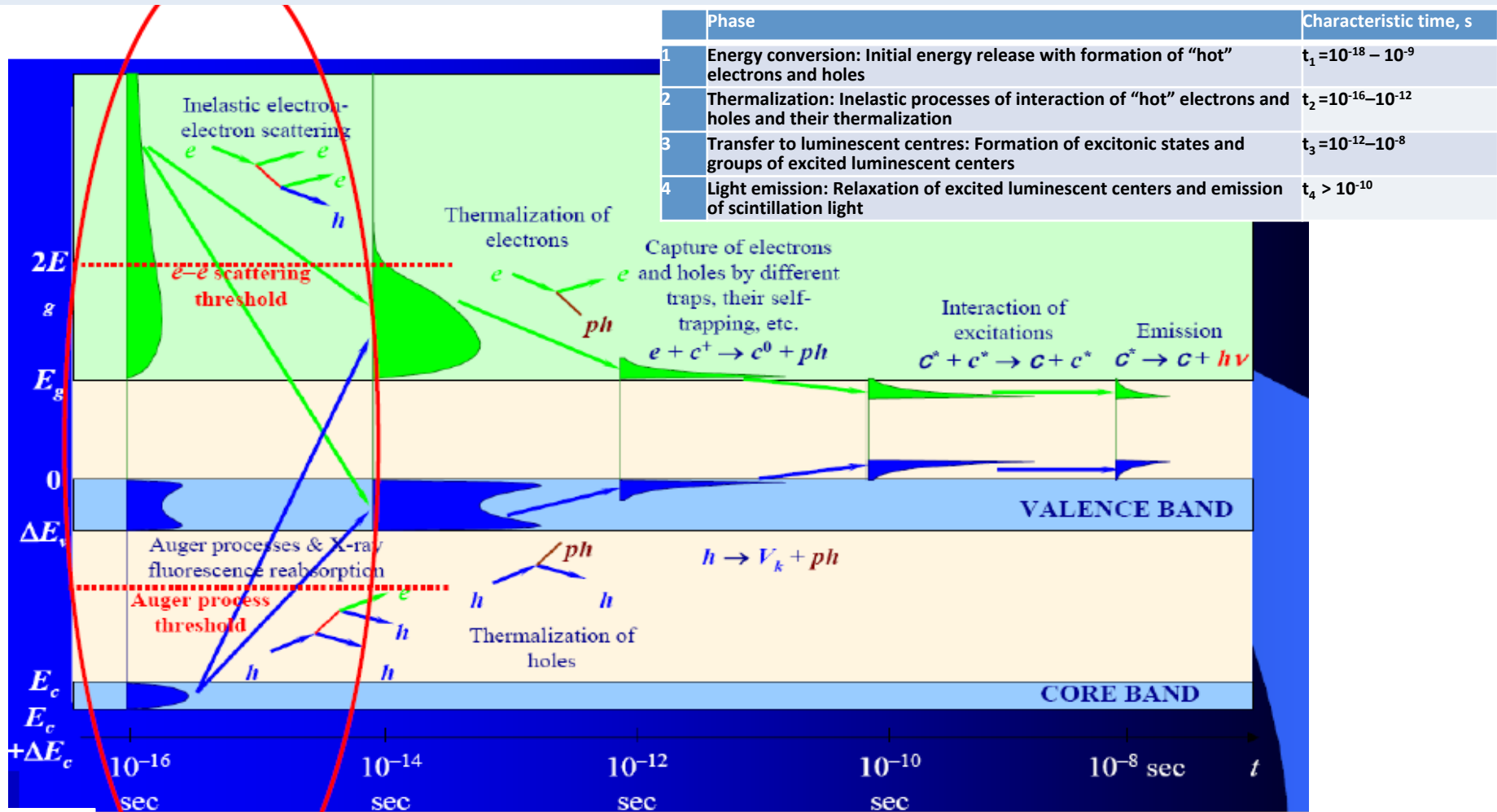
Barrel: 11300 Endcaps: 3864crystals

New big projects:

- CMS BTL at HL LHC
- LHCb upgrade at HL LHC
- FCC (e-e)
- Brookhaven Ion-e collider



Development of scintillation in a dielectric material

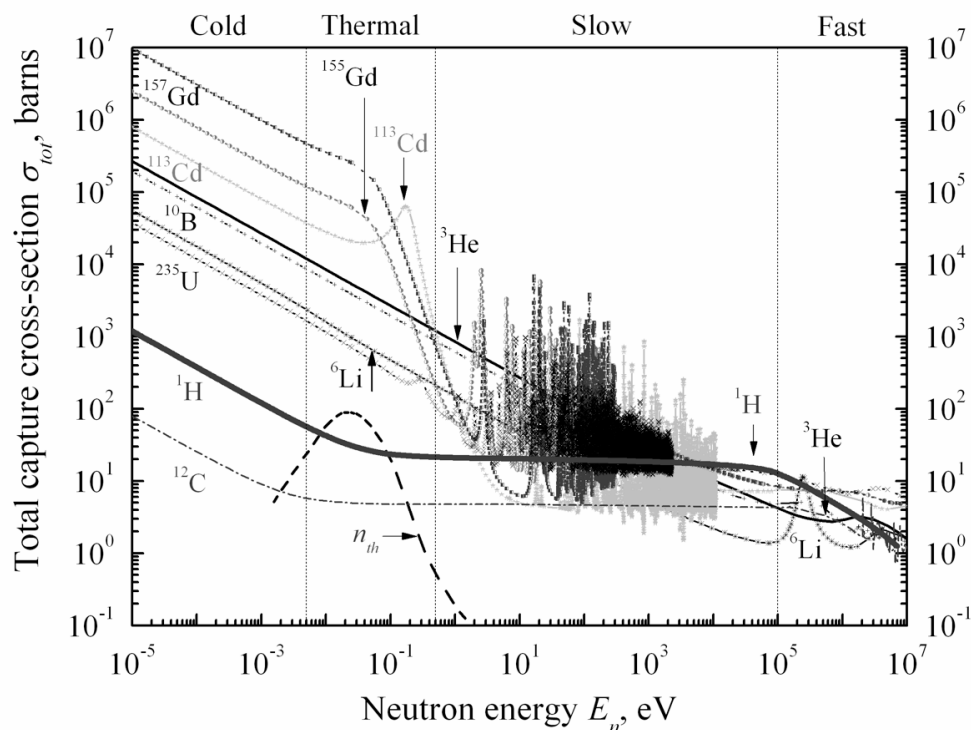


Developing of excitation in space:
 -volume with radius about 0.5 micron
 around trajectory

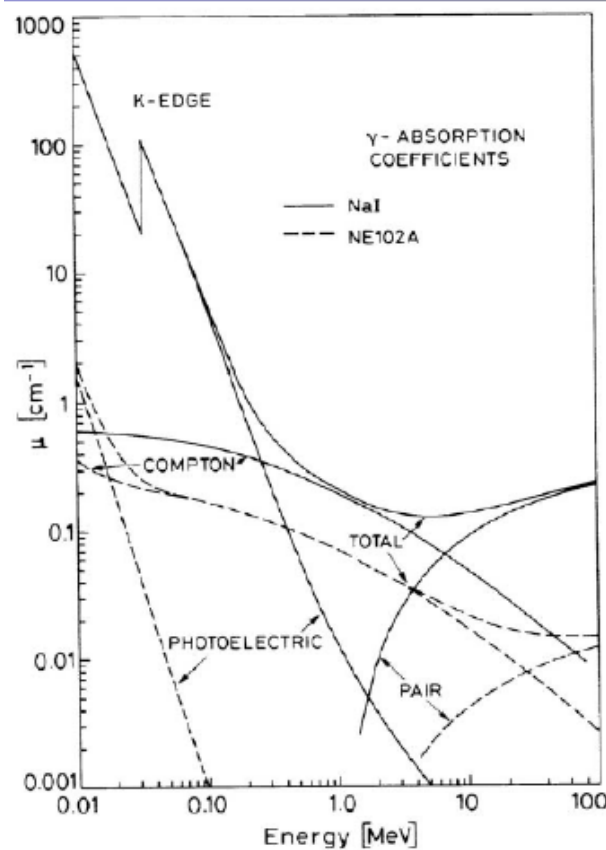


Interaction of neutrons with nuclei of some elements

Interaction of gamma-quanta with matter



isotope	CROSS-SECTION OF THERMAL NEUTRON ABSORPTION, BARN	NATURAL ABUNDANCE, %
³ He	5.4×10^3	0.000137
⁶ Li	0.9×10^3	7.59
¹⁰ B	3.8×10^3	19.9
¹¹³ Cd	2×10^3	12.22
¹⁵⁵ Gd	6×10^4	14.8
¹⁵⁷ Gd	2.5×10^5	15.65



- Photoelectric: $\sigma_{ph} \propto \frac{Z^5}{E_\gamma^{7/2}}$
- Compton: $\sigma_c \propto Z$
- Pair production: $\sigma_{pair} \propto Z^2 \ln(2E_\gamma)$



Parameters of scintillation

Scintillation yield: $Y = \frac{E_\gamma}{\beta E_g} SQ$ (In a case of gamma-quanta)

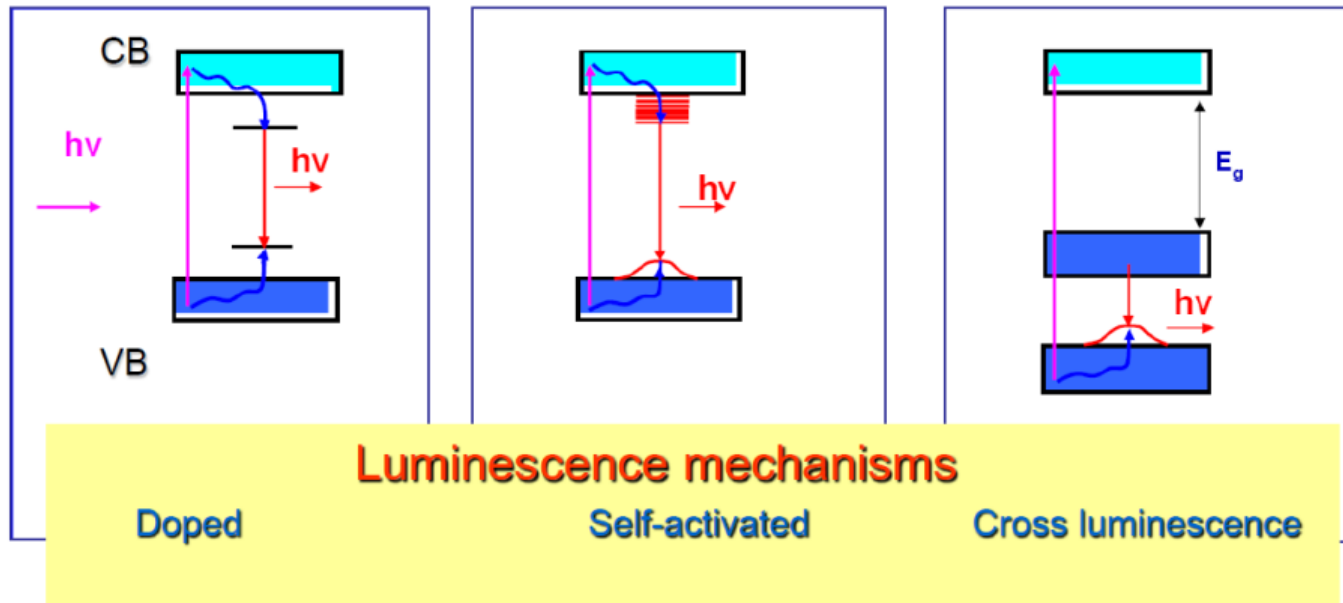
Kinetics of scintillations: The kinetics of scintillation $I(t)$ is defined as the law of time variation of the scintillation light intensity, and its magnitude $I = \int I(t) dt$ is proportional to Y .

Radio-luminescence spectrum: This is the wavelength (or frequency/energy) distribution of the scintillation light when the medium is excited by ionizing radiation.

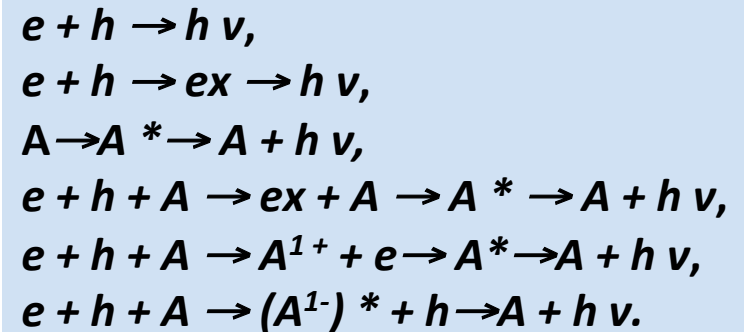
Photo-luminescence spectrum: This is the wavelength (or frequency/energy) distribution of the scintillation light when the medium is excited by photons of energy below the ionization energy of the atoms.



Classification of the luminescence mechanisms



Mechanisms of the luminescence creation.



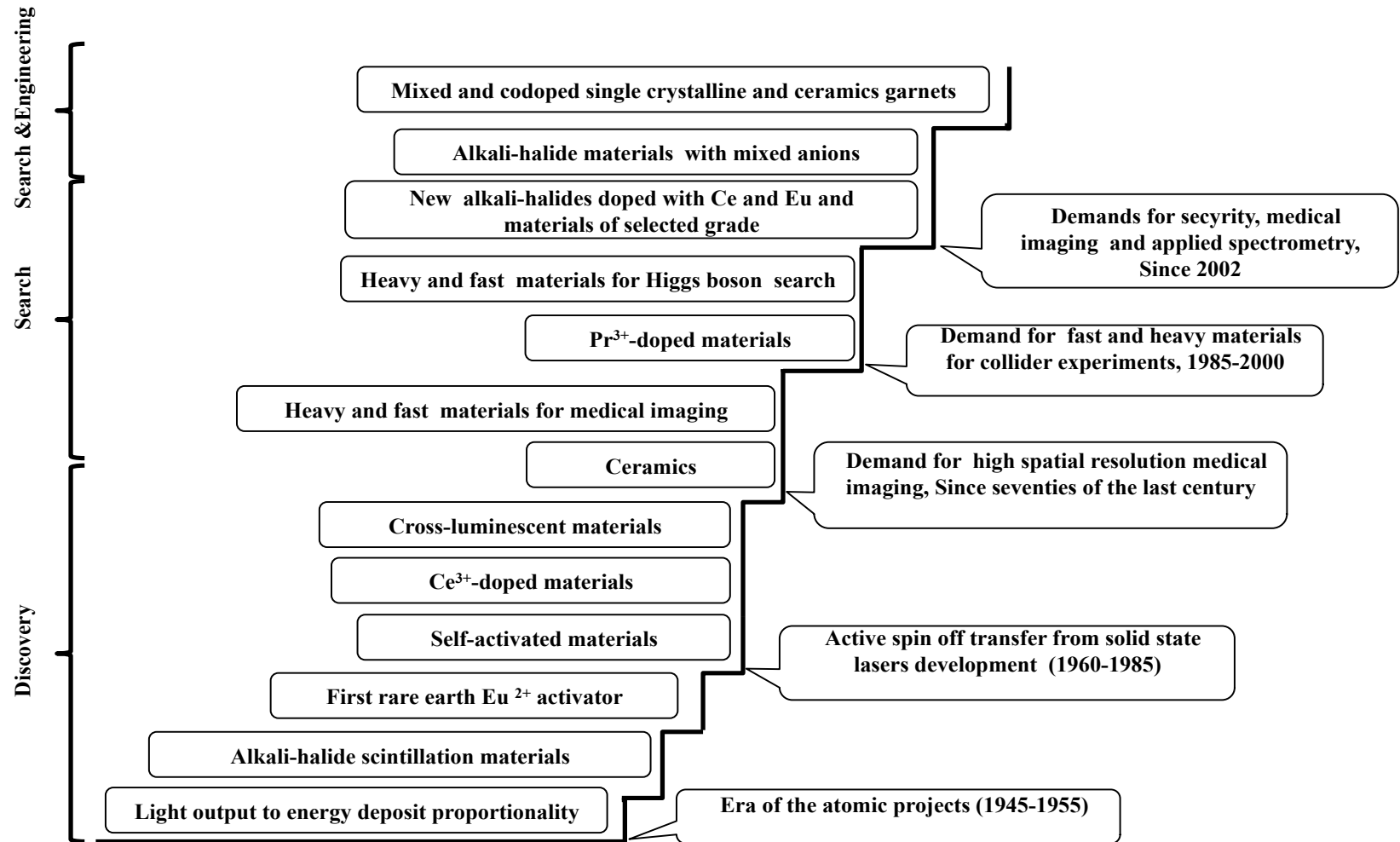
Classification of the scintillation materials

Scintillator	ρ , g/cm ³	$Z_{\text{eff}}/\text{photo}$ absorp. coeff., 511 keV, cm ⁻¹ / X_0 , cm	Y , ph/MeV	τ_{sc} , ns	λ_{max} , nm	Ref.
Fluorides						
Cross-luminescent materials						
LiBaF ₃	5.2	49/0.079/2.1	1400	0.8	190, 230	107
KMgF ₃	3.2	14.3/0.0007/8.4	1400	1.3	140–190	107
KCaF ₃	3	16.7/0.001/7.7	1400	2	140–190	107
KYF ₄	3.6	30/0.011/4.6	1000	1.9	170	107
BaLu ₂ F ₈	6.94	63/0.22/1.25	870	1+slow	313	108, 109
BaF ₂	4.88	53/0.085/2	1430	0.6	220	110
			9950	620	310	
CsF	4.64	53/0.086/2.7	1900	2–4	390	111
RbF	3.6	35/0.016/3.6	1700	1.3	203, 234	107
Self-activated materials						
CeF ₃	6.16	53/0.11/1.8	4500	30	330	112, 113
Activated						
BaY ₂ F ₈ :Ce	4.97	44/0.04/2.5	980	45+slow	329	108, 109
BaLu ₂ F ₈ :Ce	6.94	63/0.22/1.35	400	35+slow	330	108, 109
CaF ₂ :Eu	3.18	16.4/0.045/3.7	21 500	940	435	114
LaF ₃ :Ce	5.9	50.8/0.09/1.7	2200	26.5	290, 340	115
LuF ₃ :Ce	8.3	61/1/0.31/1.1	8000	23+slow	310	115

More details in: P. Lecoq, A. Gektin, M. Korzhik, Inorganic Scintillators for Detector Systems, Springer 2017, P.408

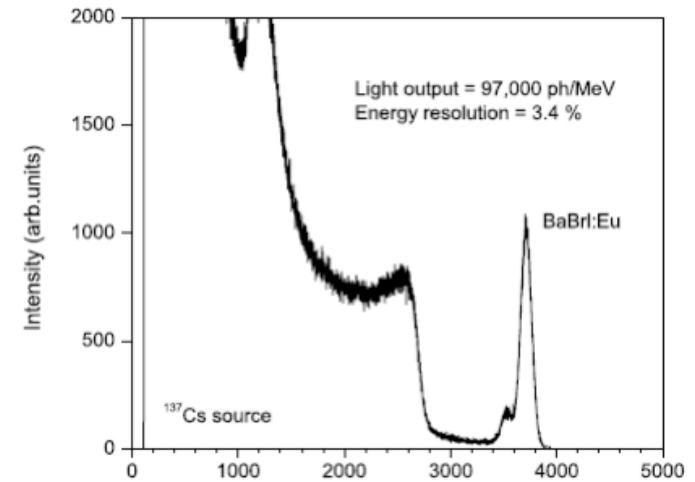


The story of the scintillation materials

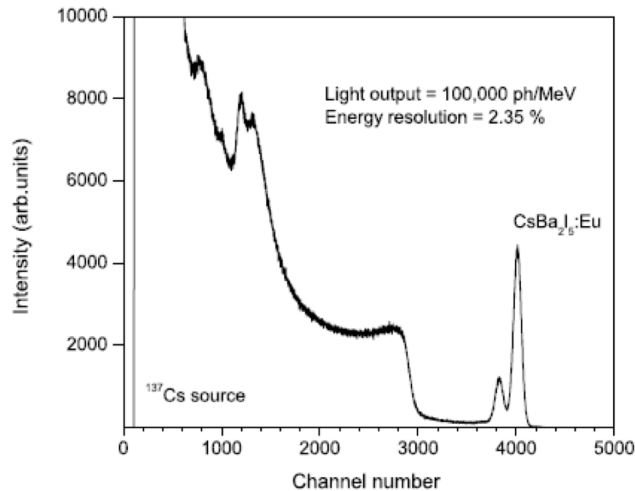


Major trends and results. New Eu doped alkali halides

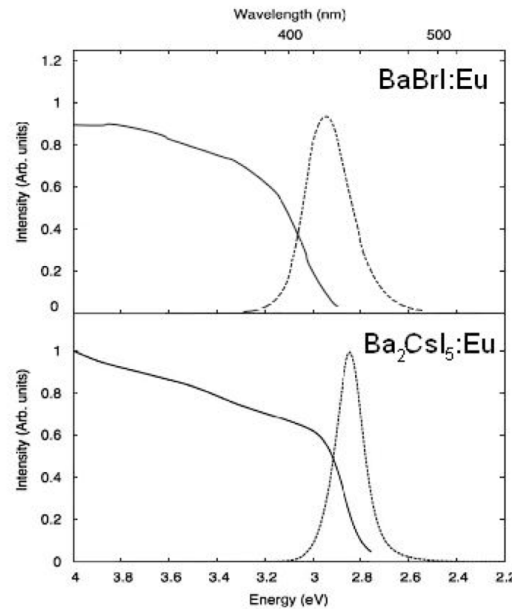
Crystal	ρ g/cm ³	Lum λ , nm	LY ph/MeV	R, % Cs ¹³⁷	Decay, ns	Hygroscopicity
CaI ₂ :Eu ²⁺	3.96	467	110.000	5,2	1000	strong
SrI ₂ :Eu ²⁺	4.55	435	115.000	2.6	1500	strong
Ba ₂ CsI ₅ :Eu ²⁺	4.9	435	102.000	2.55	383; 1500	medium
SrCsI ₃ :Eu ²⁺	4,25	458	73.000	3.9	2.200	medium
BaBrI:Eu ²⁺	5.2	413	97.000	3,4	500	low
LaBr ₃ :Ce ³⁺	5.3	356, 387	75.000	2,6	16	strong



Pulse height spectra of BaBrI:Eu scintillators (137 Cs source)



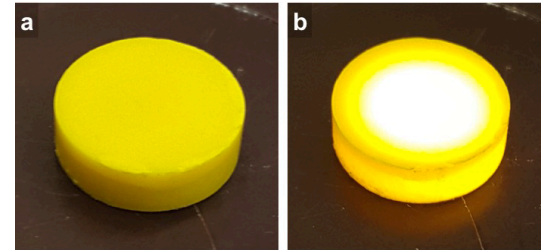
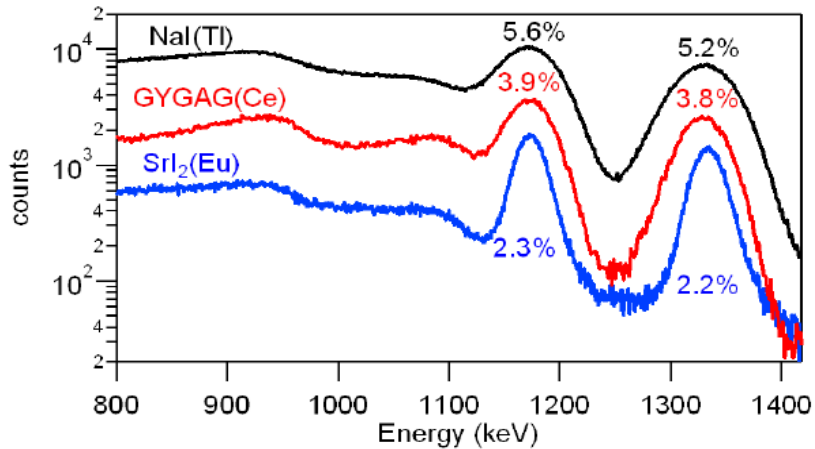
Pulse height spectra of CsBa₂I₅:Eu scintillators (137 Cs source)



Overlapping of absorption and luminescence spectra of Eu²⁺ in alkali halides



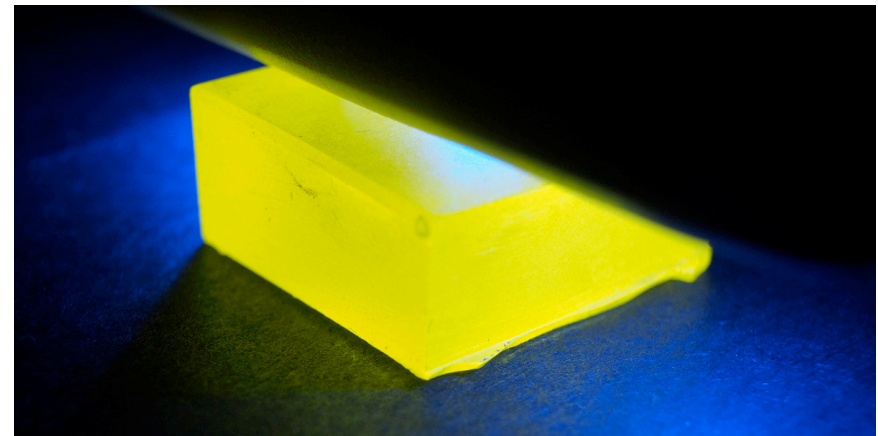
Mixed crystals



First GYAGG ceramics, obtained in NRC “Kurchatov Institute”

Scintillation parameters of main elpasolites for neutron detection

	CLYB	CLYC	CLLC	CLLB	CLLBC
Light yield,					
gamma, ph/MeV	24 000	20 000	35 000	45 000	45 000
neutron, n/MeV	90 000	70 000	110 000	150 000	150 000
ER, % @ 662 keV	4.1	4.0	3.4	2.9	3
Emission, nm	410	370	380	410	410



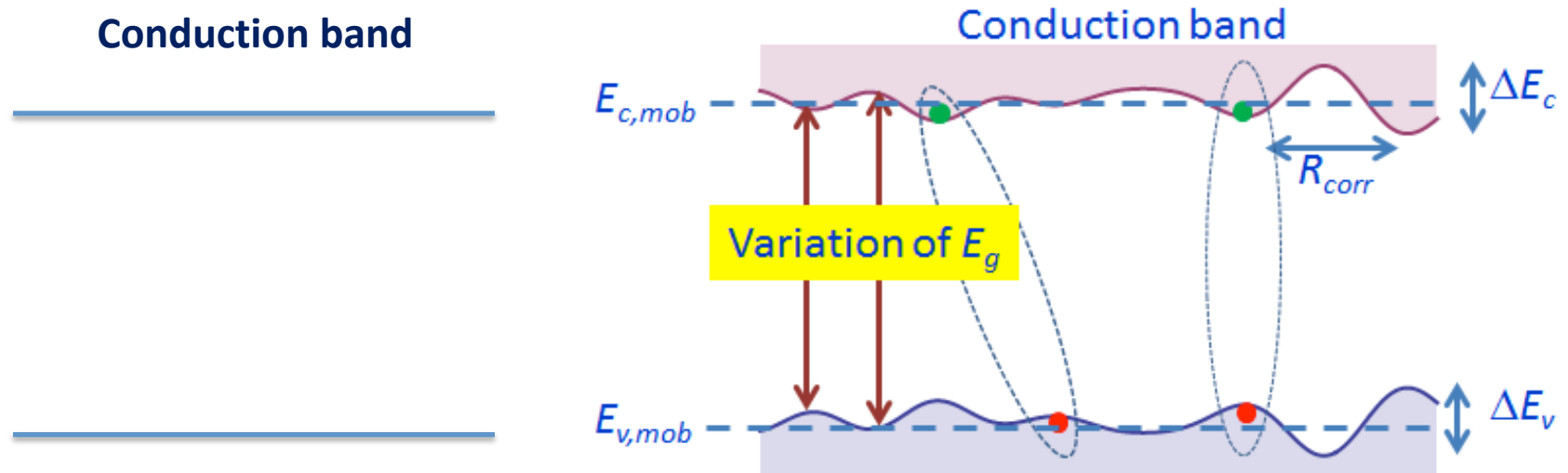
First GAGG crystal, was grown in Russia

Toward the multicomponent materials for scintillators!

Toward the best time resolution.

Binary crystalline systems versus mixed crystals

Engineering of scintillation materials



Valence band

Binary crystal

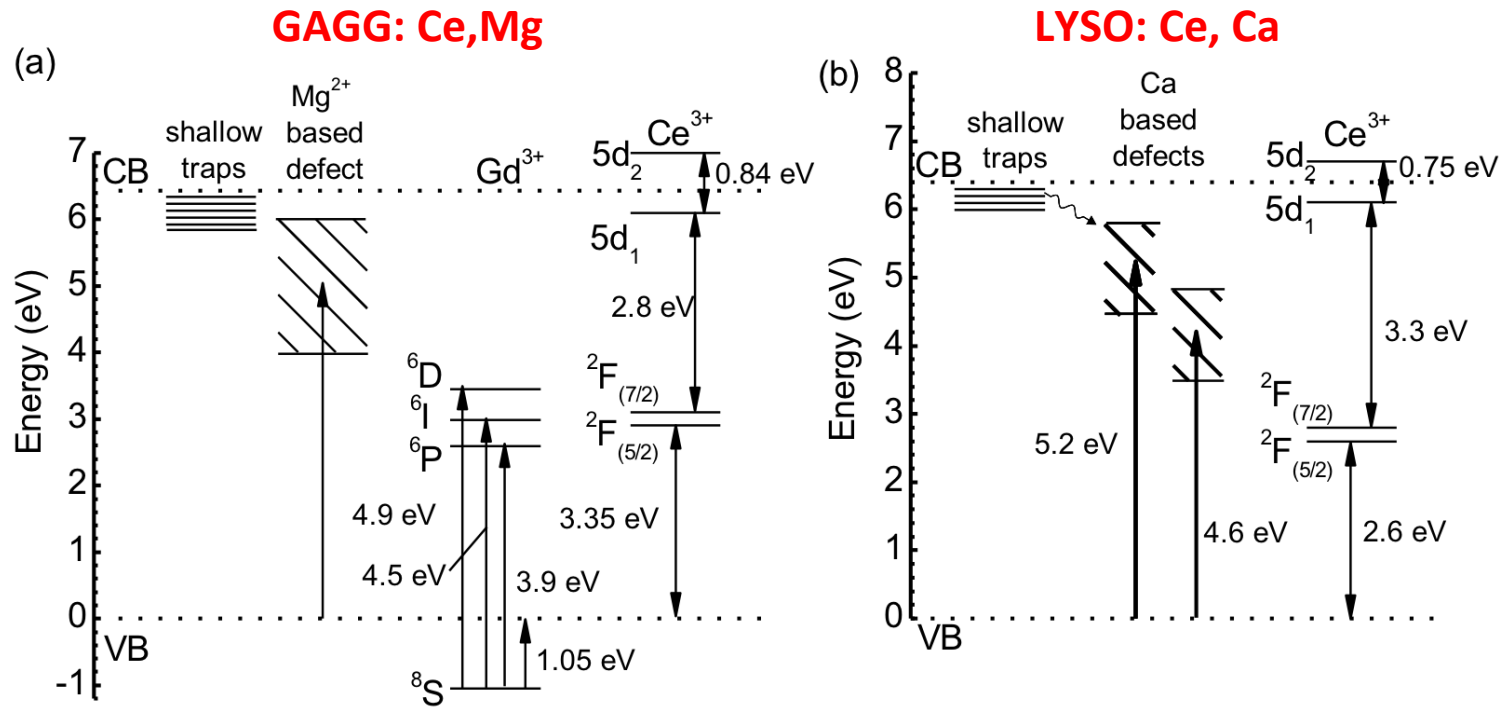
Flat bottom of the conduction band.
Fast migration of excitations.

Mixed crystal with band gap fluctuations

Modulated due to disordering bottom of the conduction band. Slower migration of excitations.

Engineering of electronic excitations transfer process

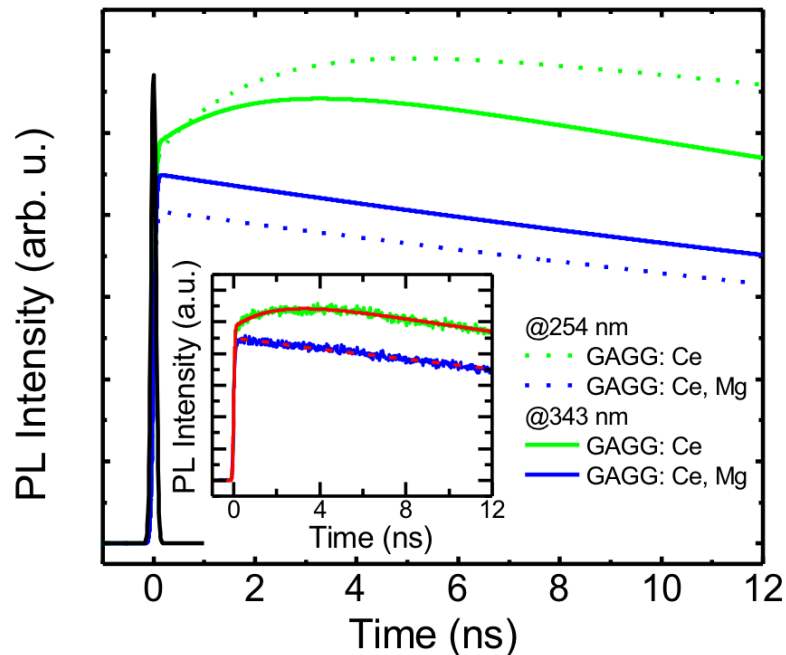
Need for appropriate codoping in mixed GAGG and LYSO crystals



Energy-level diagram for GAGG crystal doped with Ce and codoped with Mg (a) and for LYSO doped with Ce and codoped with Ca (b)

Control of scintillation rise time

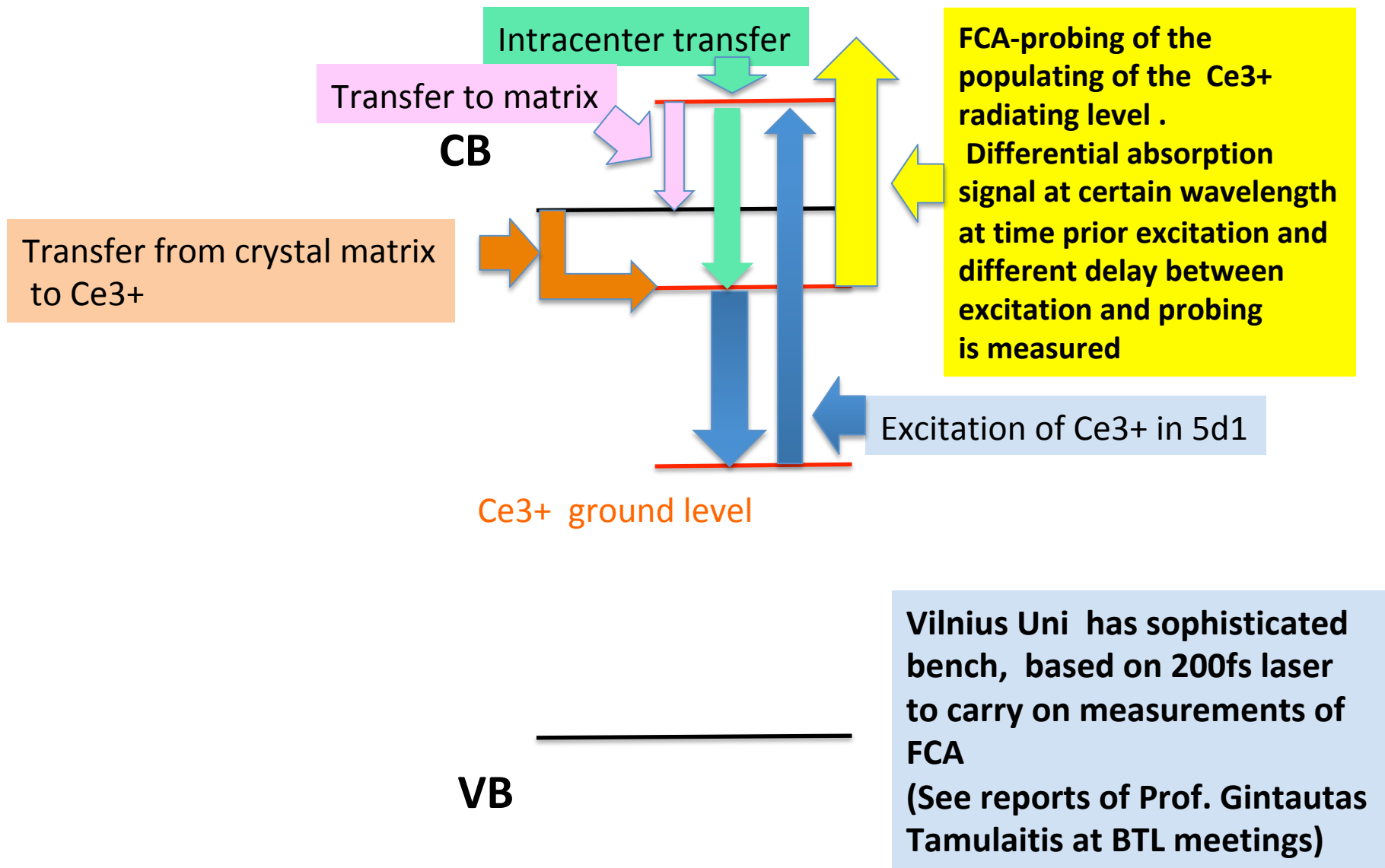
Ce^{3+} luminescence rise in GAGG solely doped with Ce and codoped with Mg



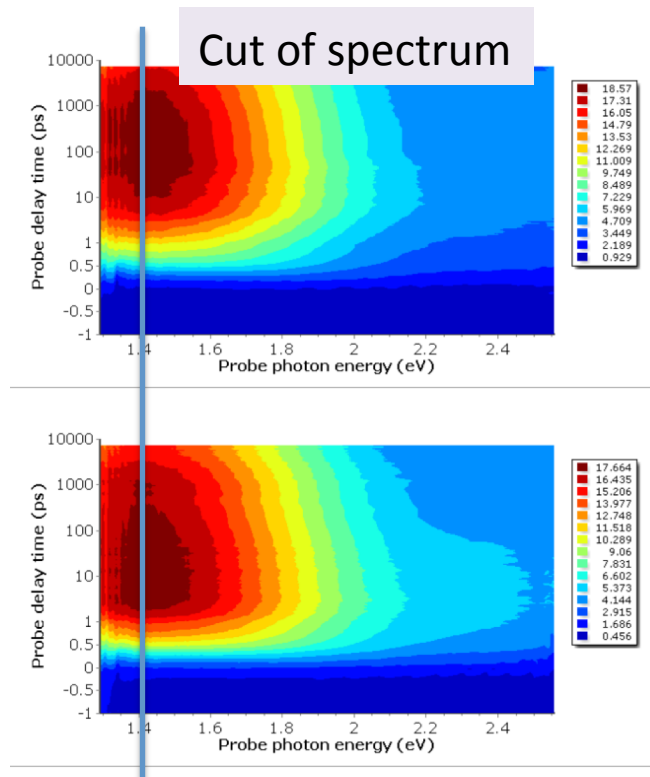
The initial part of photoluminescence response to a short excitation pulse at 343 nm in GAGG:Ce without (green) and with Mg codoping (blue). Instrumental response function is also presented

M. Korzhik, G.Tamulaitis et al. Excitation transfer engineering in Ce-doped oxide crystalline scintillators by codoping with alkali-earth ions, *phys. stat. solidi (a)*, 1700798 (2018)

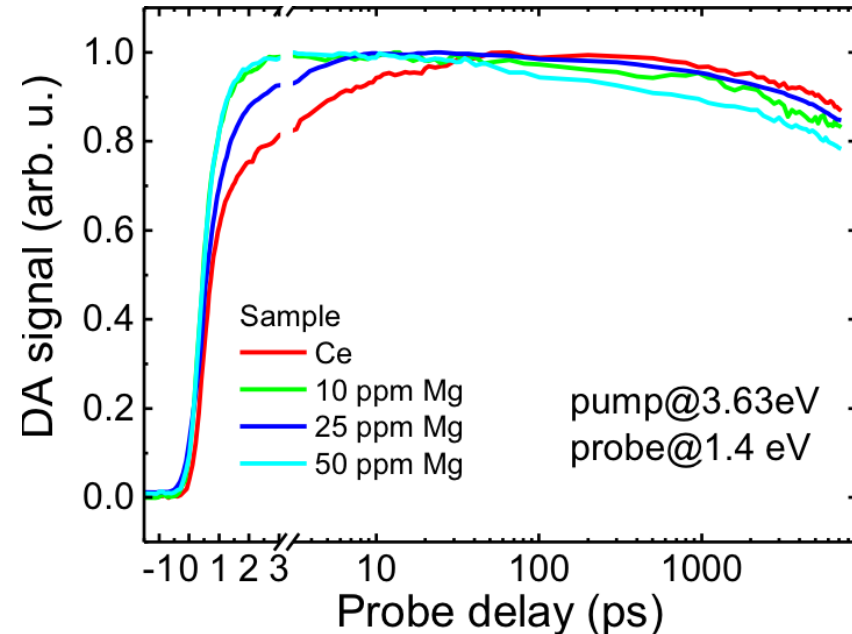
Probing of the nonequilibrium carriers absorption in dielectrics



Dynamics of the populating of radiating level of Ce³⁺ in GAGG crystal



Differential absorption of Ce-doped (a) and Ce,Mg-codoped (b) GAGG as a function of probe photon energy and delay between pump and probe pulses at pump photon energy of 3.63 eV. Note the scale change from linear to logarithmic at 1 ps.



Differential absorption kinetics at 1.4 eV of GAGG samples with different level of codoping pumped at 3.63 eV



Materials of interest: scintillators on a base of Ce-doped inorganic crystalline oxides

Most of the oxides are multifunctional materials:

- have applications in medical imaging and industry;
- technology is well developed, a few suppliers are available for each crystal
- technology is well developed, no additional investment is required;
- easy handled and radiation tolerant

Scintillator	ρ , g/cm ³	Z_{eff} /photo absorp. coeff., 511 keV, cm ⁻¹ / X_0 , cm	Y, ph/MeV	τ_{sc} , ns	λ_{max} , nm
Gd ₃ Al ₂ Ga ₃ O ₁₂ :Ce	6.67	50.6/0.12/1.61	46,000	80 800	520
(GdY) ₃ (Al-Ga) ₅ O ₁₂ :Ce	5.8	45/0.08/1.94	60,000	100,600	560
Y ₃ Al ₅ O ₁₂ :Ce	4.55	32.6/0.017/3.28	11 000	70	550
YAlO ₃ :Ce	5.35	32/0.019/2.2	16 200	30	347
(Y _{0.3} -Lu _{0.7}) AlO ₃ :Ce	7.1	60/0.21/1.3	13 000	18/80/450	375
Lu ₂ SiO ₅ :Ce	7.4	66/0.28/1.1	27 000	40	420
(Lu-Y) ₂ SiO ₅ :Ce	7	60/0.20/1.35	30 000	37	420

More details in: P. Lecoq, A. Gektin, M. Korzhik, Inorganic Scintillators for Detector Systems, Springer 2017, P.408



MIP detection

Ionization losses per 1 mm of the media for 10GeV e^- and 50Gev π^-

Material	Density ρ , g/cm ³	dE/dx @ e^- , MeV/mm	dE/dx @ π^- , MeV/mm
Plastic scintillator (vinyltoluene based)	1.032	0.154	0.154
$Y_3Al_5O_{12}$ (YAG)	4.55	0.591	0.589
$Y_3(Al_{0.5}Ga_{0.5})_5O_{12}$	4.80	0.614	0.612
$YAlO_3$ (YAP)	5.50	0.708	0.705
$Gd_3Al_2Ga_3O_{12}$ (GAGG)	6.63	0.808	0.804
Lu_2SiO_5 (LSO)	7.4	0.879	0.873
$(Lu_{0.8}Y_{0.2})_2SiO_5$ (LYSO)	7.2	0.85	0.85

Light output per MIP (10GeV e^-) per 1 mm in different scintillation materials

Material	LY, Ph/MeV	dE/dx @ e^- , MeV/mm	Yield, ph per 1 mm per MIP
Plastic scintillator (vinyltoluene based)	10000	0.154	1540
$Y_3Al_5O_{12}$ (YAG)	11000	0.591	6500
$Y_3(Al_{0.5}Ga_{0.5})_5O_{12}$	30000	0.614	18420
$YAlO_3$ (YAP)	16000	0.708	11350
$Gd_3Al_2Ga_3O_{12}$ (GAGG)	46000	0.808	37200
Lu_2SiO_5 (LSO)	27000	0.879	23700
$(Lu_{0.8}Y_{0.2})_2SiO_5$ (LYSO)	30000	0.85	25500

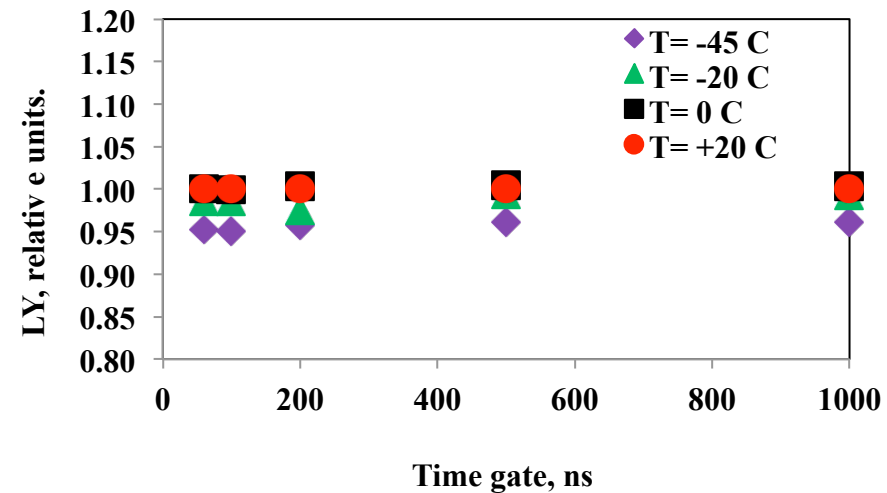
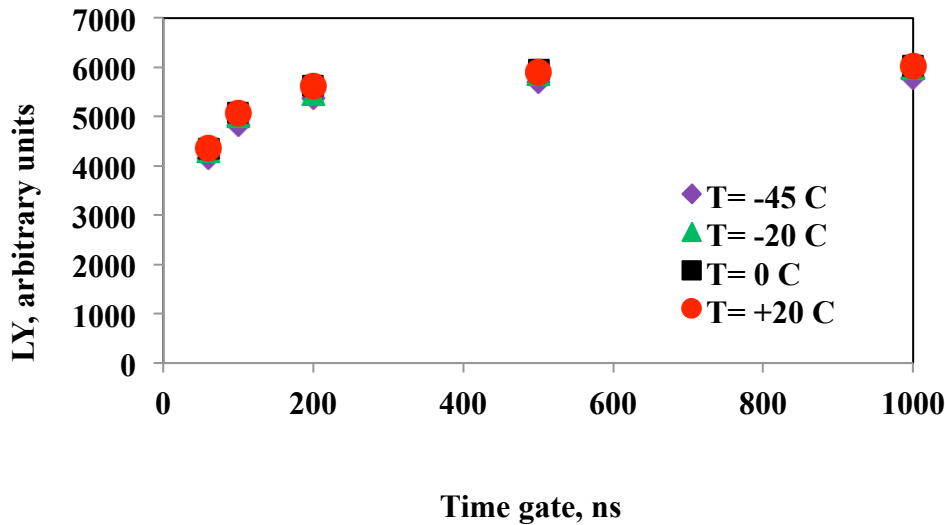
Time and energy resolution at 511keV

Crystal	Time resolution CTR at 511 keV, FWHM, ps
GAGG:Ce	480
GAGG:Ce, Mg	200
GAGG:Ce, Mg, Ti	155
LYSO:Ce	130
LSO:Ce	122
LYSO:Ce, Ca	95
LuAG:Ce	530
LuAG:Ce, Ca	230
LuAG:Pr	300

T, °C	+20	0	-20
GAGG:Ce, Mg, Ti Energy resolution at 511 keV, % FWHM	7,2	7,0	6,8
LYSO:Ce, Ca Energy resolution at 511 keV, % FWHM	8,2	8,3	8,6

Light yield at different temperatures.

LSO gated light yield at different T

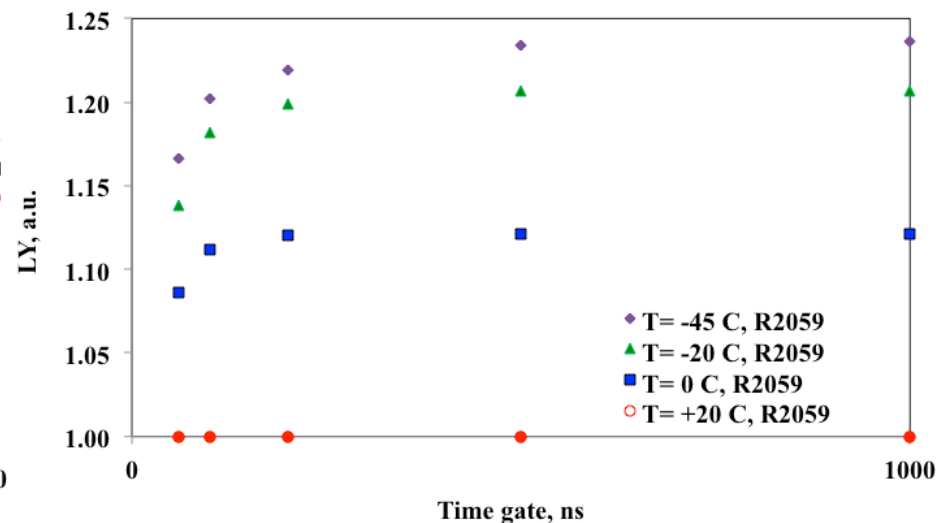
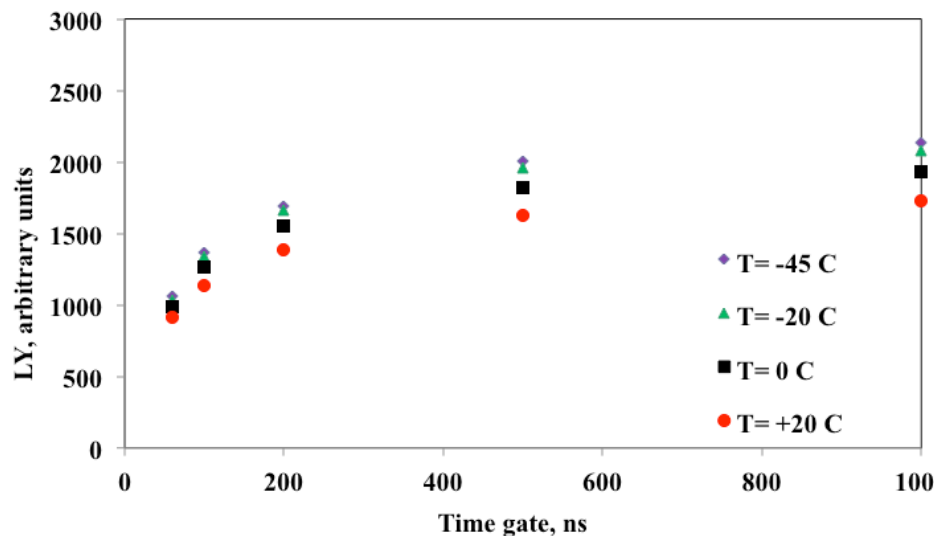


LSO:Ce light yield measured within different time gates in the temperature range from +20 to -45°C. Sample size 10x10x1 mm³

LSO:Ce light yield normalized to that at 20°C, measured within different time gates in the temperature range from +20 to -45°C. Sample size 10x10x1 mm³

Light Yield at different temperatures.

GAGG:e, Mg, Ti gated light yield at different T



GAGG light yield measured within different time gates in the temperature range from +20 to -45°C.

Sample size 10x10x1 mm³

GAGG light yield normalized to that at 20°C, measured in different time gates in the temperature range from +20 to -45°C.

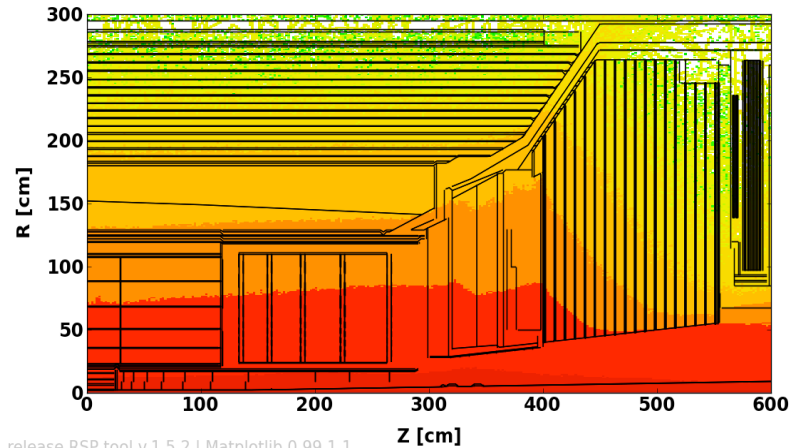
Sample size 10x10x1 mm³

V.Korjik, V.Alenkov, et.al., NIM A 871(2017)42-46

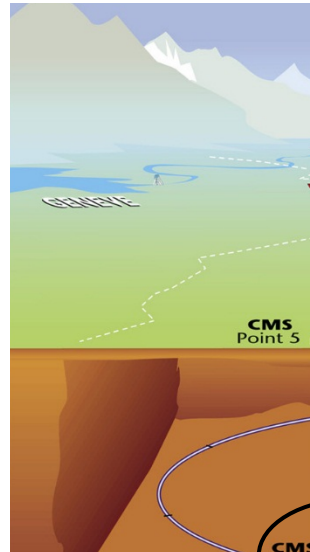
Toward an increase the luminosity of LHC

CMSphase2 pp 7TeV v3.7.0.0 FLUKA:
Protons (Central Region, Tracker+Calorimeters)
3000.0 [fb⁻¹]

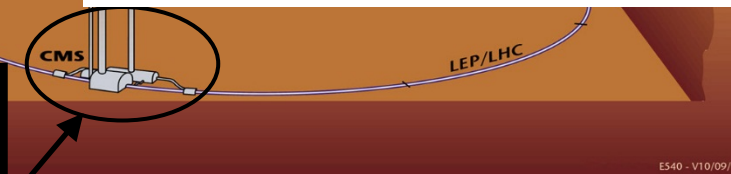
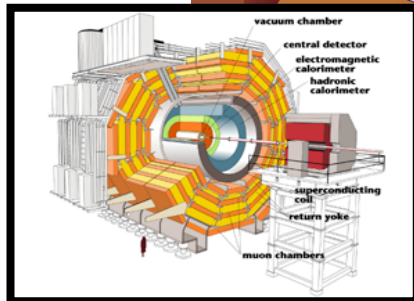
for internal CMS use only



release RSP tool v.1.5.2 | Matplotlib 0.99.1.1
simulation author: BRIL Rad Sim



CMS



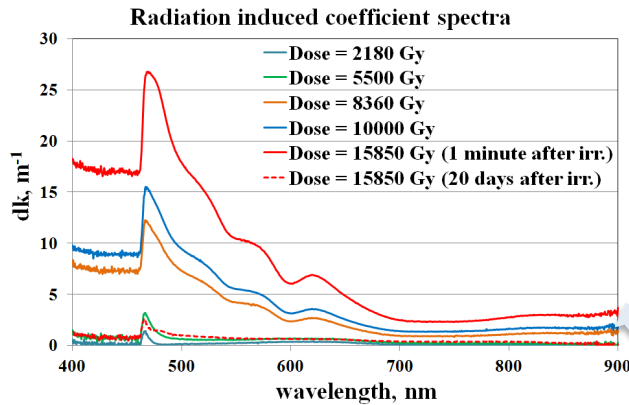
E540 - V10/09/97



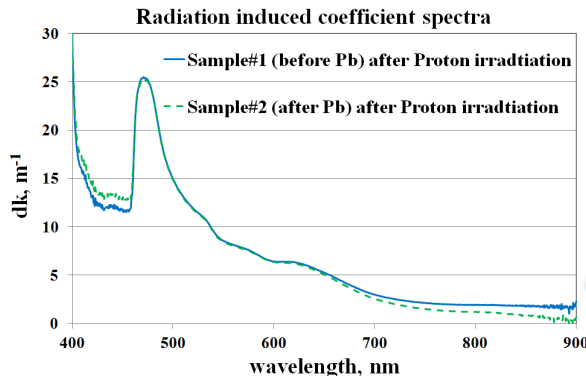
Global trend in modern collider experiments: to replace plastic scintillators by more radiation hard materials

Essential problems of the plastic matrix:

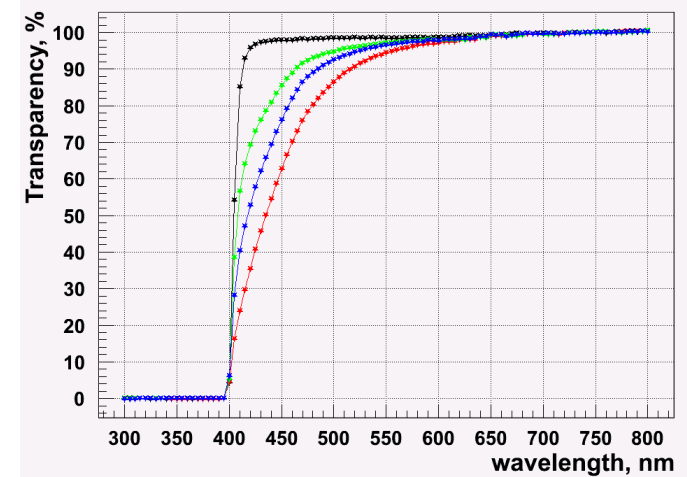
- damage under irradiation by hadrons and the products of nuclear reactions;
- low energy deposit by MIPs



Induced absorption in EJ200 after irradiation at RT with ^{60}Co at different exposed doses



Induced absorption in EJ200 after irradiation with KVI (Groningen) at the fluence of $5 \cdot 10^{13} \text{ p/cm}^2$

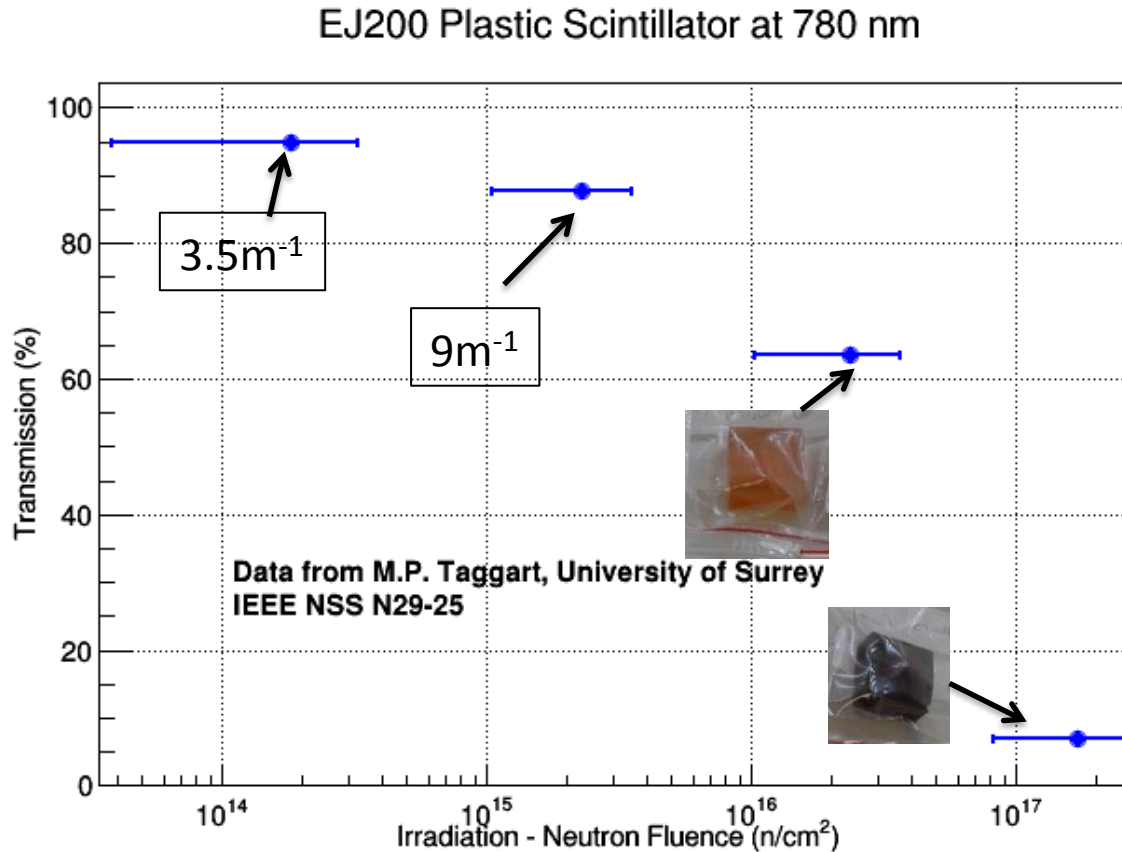


Polystyrene BASF 165 H+1.75%PTP+0.05% POPOP, $h = 3 \text{ mm}$, 24 GeV protons: $5 \cdot 10^{14}$ (green), blue- $1.3 \cdot 10^{15}$ (blue), red- $3.1 \cdot 10^{15} \text{ p/cm}^2$ (red).
Courtesy of LHCb Collaboration at CERN

V.Dormenev, K.T.Brinkmann, M.Korjik et al., Journal of Physics: Conference Series 928 (1), 012035

IRRADIATION WITH FAST NEUTRONS

Essential difference from the damage under protons – induced light scattering come up!



Impact of radiation damage effects from different components of ionizing radiation on energy resolution of ECAL detecting module

$$a_{phot} = \sqrt{\frac{F}{LY}}$$

$$b \sim \frac{\text{Noise (electrons)}}{LY \left(\frac{pe}{MeV}\right)}$$

$$c \sim \frac{1}{LY} \frac{\partial LY}{\partial z} \delta z$$




$$\frac{\sigma(E)}{E} = \frac{a}{\sqrt{E}} \oplus \frac{b}{E} \oplus c$$

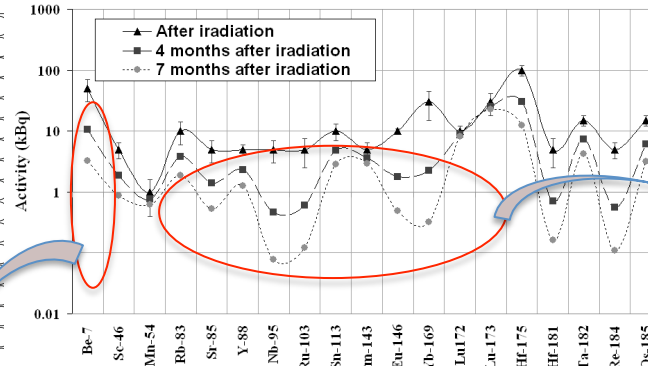
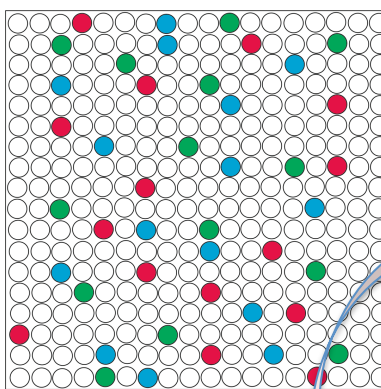
Time resolution deterioration & photo receivers loading due to parasitic radio-luminescence from radio-isotopes

	Essential effects	γ- quanta	Charged hadrons	Neutral hadrons
1	Change of the thermodynamic equilibrium due to creation of colour centers	✓	✓	✓
2	Creation of new defects and dedicated colour centers	+/-	✓	✓
3	Creation of non recoverable damages		✓	✓
4	Change of the material composition due to nuclear reactions (radio isotopes and fragments)		✓	✓

Damage under ionizing radiation

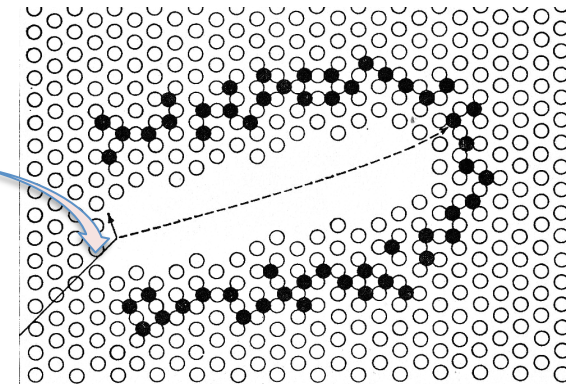
Point defects due to crystal growth

-  $-V_A$
-  $-V_C$
-  Interstitial sites



Set of isotopes identified in PWO crystal : measured activity 4 months after irradiation and the extrapolated values at 24 h and 7 months after the end of irradiation.

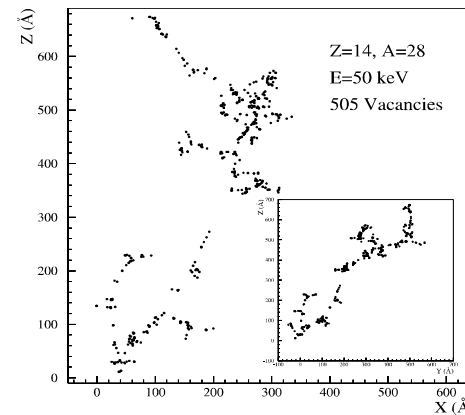
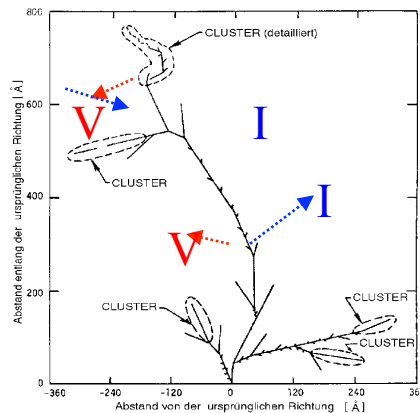
Stars created by fission products



L.T.Chadding, 1965

Point defects and their clusters which are created by knocked ions

Van Lint
1980



M.Huhtinen
2001

List of the scintillation materials studied

γ-quanta
60Co(1.22MeV),
absorbed doses 10-2000Gy

24 GeV
&
150 MeV protons

reactor
neutrons

PWO, PWO-II

LSO:Ce(LYSO:Ce)

LuAG:Ce

BSO

PbF₂

BaF₂

GSO:Ce

YSO:Ce

YAG:Ce(Pr)

YAP:Ce (Pr)

DSB:Ce(glass and glass-ceramics)

Y₂O₃ (micro-ceramics)

LiF

PWO, PWO-II

LSO:Ce(LYSO:Ce)

LuAG:Ce

BSO

PbF₂

BaF₂

GSO:Ce

YSO:Ce

YAG:Ce(Pr)

YAP:Ce (Pr)

DSB:Ce(glass and glass-ceramics)

Y₂O₃ (micro-ceramics)

LiF

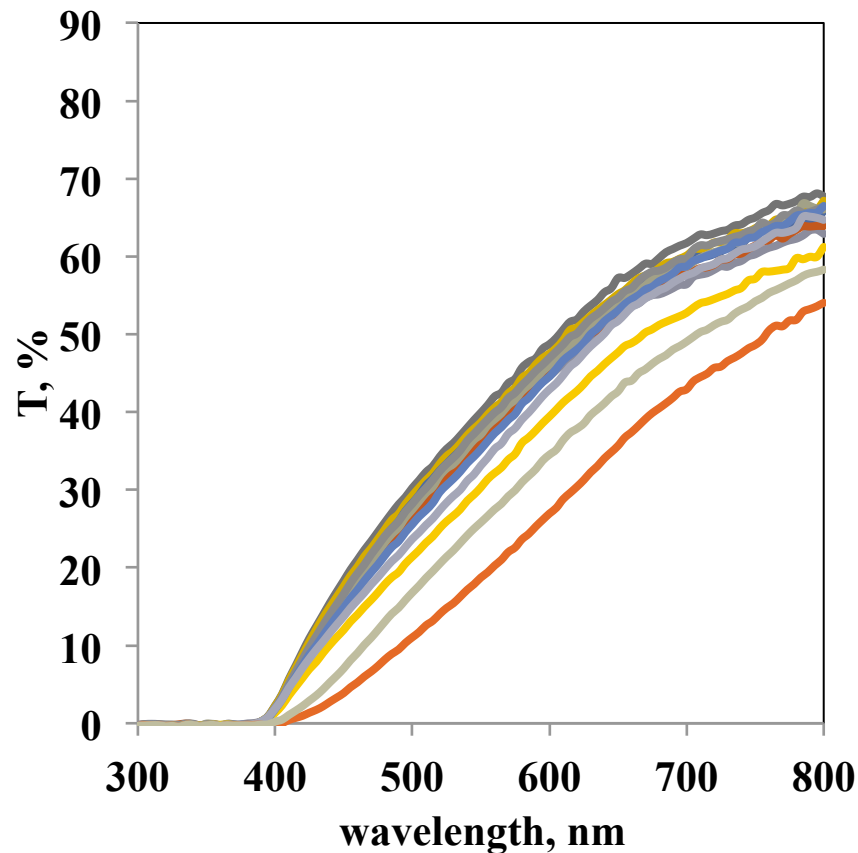
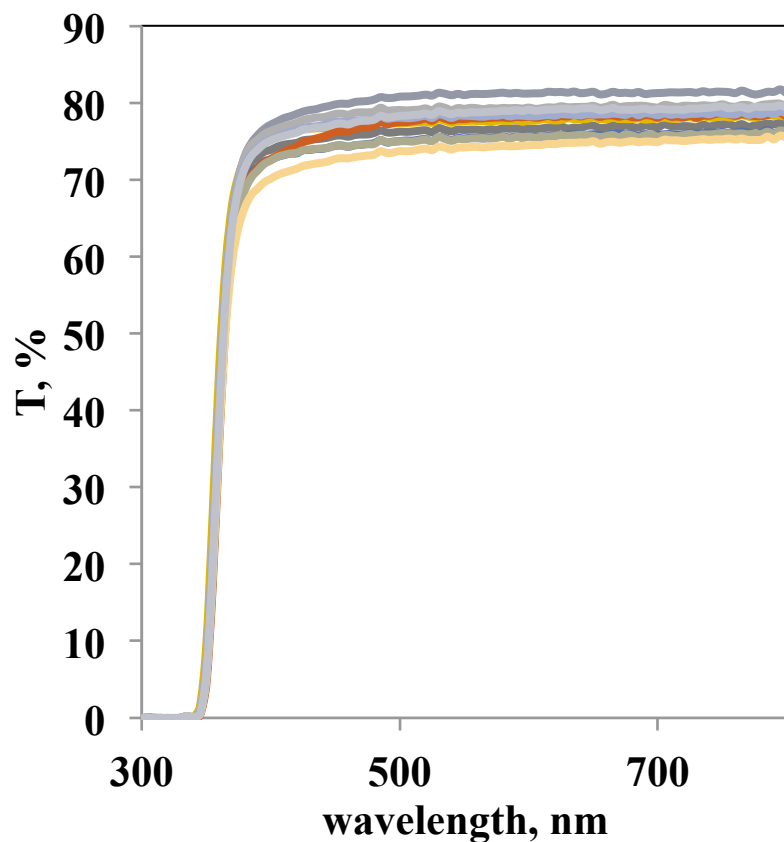
PWO, PWO-I

There is not too much of available Information up to now

May be also interesting for:

- (1) well logging tools;
- (2) Detectors at spallation sources.

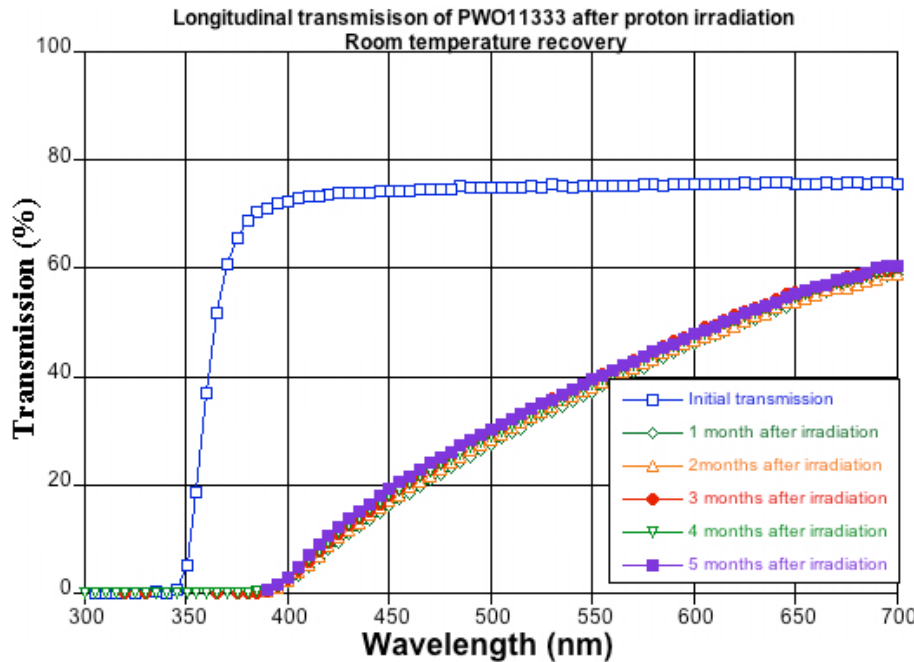
Damage of the optical transmission of PWO crystals under gamma-irradiation and high energy protons



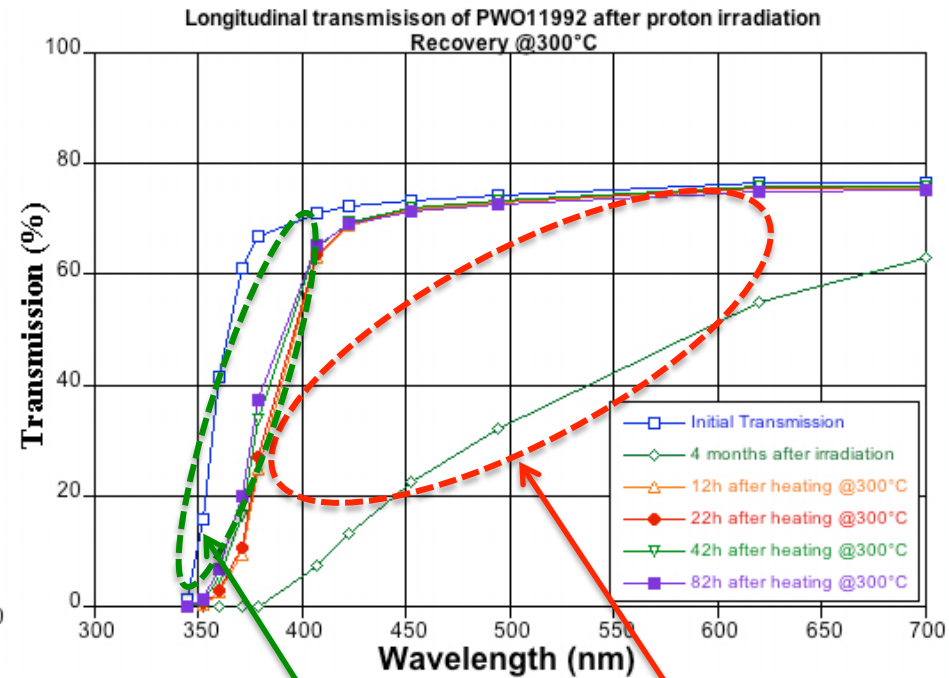
Change of the longitudinal transmission of 22 cm long PWO crystals after irradiation with γ -quanta (^{60}Co , 1000Gy) and 24GeV protons with fluence $3,6 \cdot 10^{13}$ p/cm².

Recoverable and unrecoverable damage of the optical transmission of PbWO_4 crystals under irradiation with 24GeV protons

Spontaneous



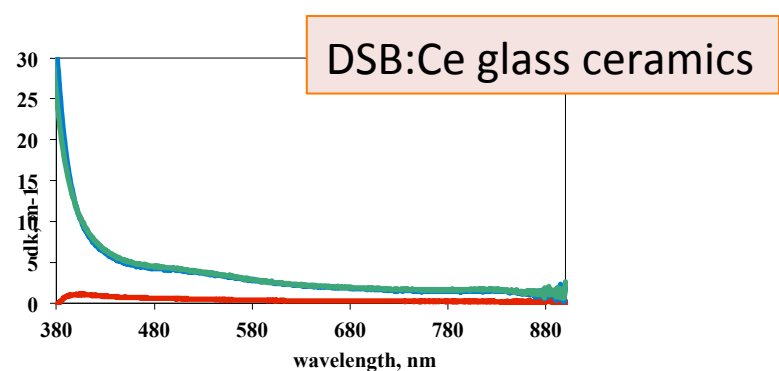
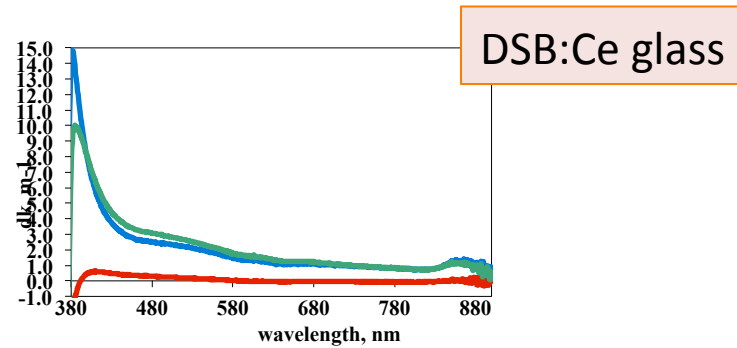
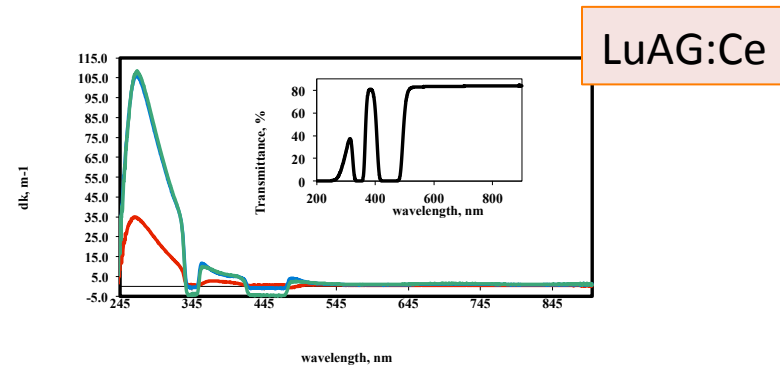
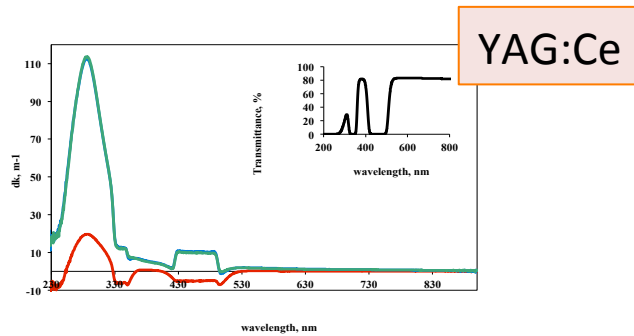
Thermally stimulated



Non recoverable part of the transmission which is caused by unrecoverable defects

Recoverable part of the transmission which is caused by single defects and clusters

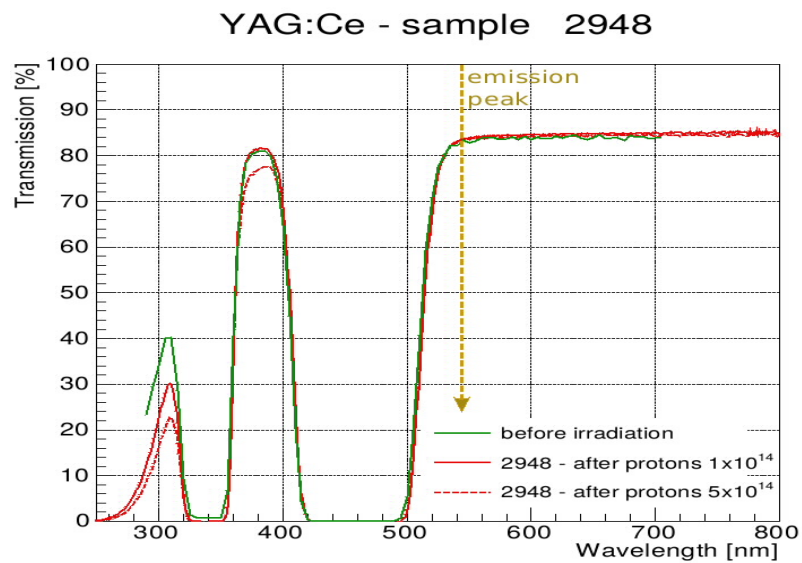
Comparison of damage of inorganic crystalline, glass and glass ceramic materials doped with Ce after irradiation with 150MeV protons and γ - irradiation



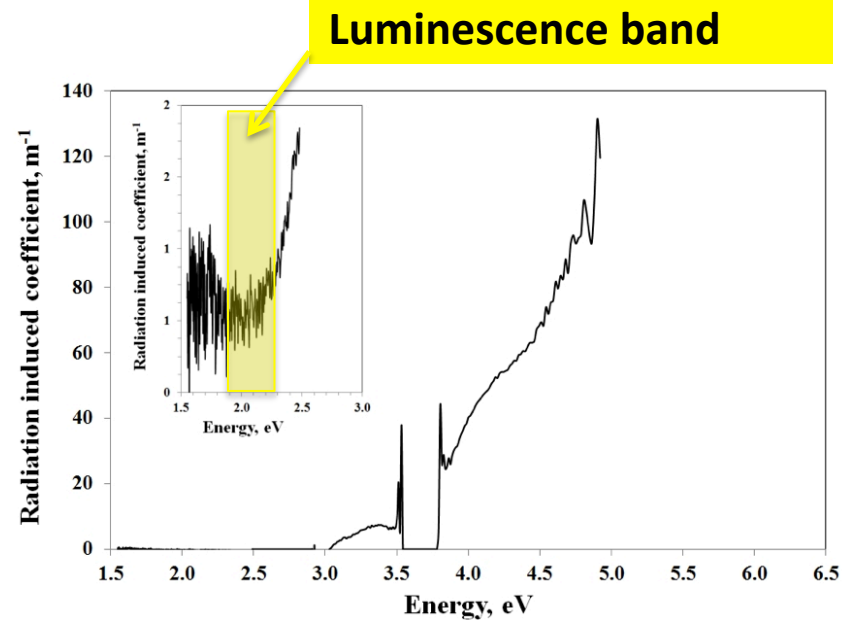
Induced absorption in several Ce doped inorganic scintillation materials:

- after γ - irradiation (^{60}Co , 1,2 MeV, 100Gy),
- in 3 months after 150 MeV proton irradiation
- repeated γ - irradiation

Garnet crystals doped with Ce^{3+} - are the most tolerant to irradiation scintillation materials

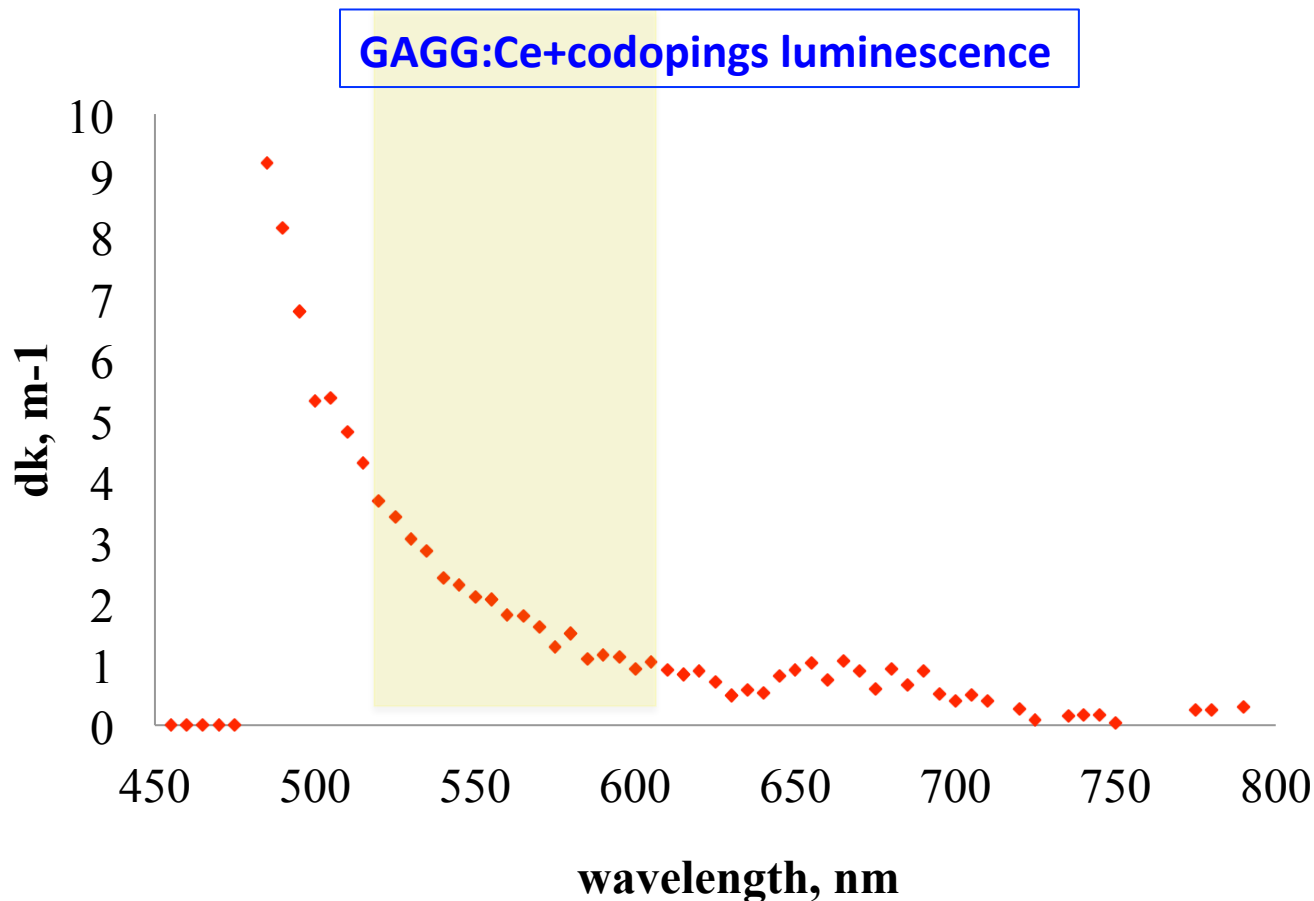


Transmission spectra of YAG:Ce 1 cm thick sample measured before irradiation and in one month after irradiation with 24 GeV protons with fluence $1 \cdot 10^{14}$ and $5 \cdot 10^{14}$ p/cm².



Proton-irradiation-induced absorption spectrum of a YAG:Ce sample, fluence $5 \cdot 10^{14}$ p/cm²

Radiation damage. GAGG:Ce+codopings induced absorption after proton irradiation



Spectrum of induced absorption in GAGG:Ce,Mg,Ti after 24 GeV proton irradiation at fluence of $3 \cdot 10^{15}$ p/cm². (Courtesy of LHCb Collaboration)

Lightweight of the material brings less radio-isotopes after irradiation with hadrons

PbF ₂			PbWO ₄		
Nuclide	Halflife, days	Activity, Bq/unit	Nuclide	Halflife, days	Activity, Bq/unit
Be-7	5,31E+01	3,12E+05	Be-7	5,31E+01	1,17E+04
Sc-46	8,38E+01	1,29E+04	Sc-46	8,38E+01	5,30E+02
			Ca-47	4,54	1,70E+02
V-48	1,60E+01	4,36E+03	V-48	1,60E+01	1,74E+02
Mn-54	3,13E+02	4,61E+03	Mn-54	3,12E+02	1,83E+02
Co-56	7,71E+01	1,57E+03			
Co-58	7,08E+01	1,37E+04	Co-58	7,09E+01	4,36E+02
Fe-59	4,46E+01	1,21E+04	Fe-59	4,45E+01	3,13E+02
Co-60	1924,889	8,80E+02			
Zn-65	2,44E+02	5,40E+03	Zn-65	2,44E+02	2,33E+02
As-74	1,78E+01	2,10E+04	As-74	1,78E+01	3,50E+02
Se-75	1,20E+02	3,99E+04	Se-75	1,20E+02	1,12E+03
Rb-83	8,62E+01	4,11E+04	Rb-83	8,62E+01	8,77E+02
			Rb-84	3,28E+01	2,21E+02
Sr-85	6,48E+01	4,85E+04	Sr-85	6,48E+01	1,38E+03
Y-88	1,07E+02	2,27E+04	Y-88	1,07E+02	5,39E+02
Zr-88	8,34E+01	3,72E+04	Zr-88	8,34E+01	1,22E+03
Nb-95	3,50E+01	4,24E+04	Nb-95	3,50E+01	4,80E+02
Zr-95	6,40E+01	1,50E+04	Zr-95	6,40E+01	2,29E+02
Ru-103	3,93E+01	4,26E+04			
Ag-105	4,13E+01	3,27E+04			
Ag-110	2,50E+02	3,15E+03			
Te-121	1,68E+01	4,32E+04	Te-121	1,68E+01	1,40E+03
Xe-127	3,64E+01	6,27E+04	Xe-127	3,64E+01	1,96E+03
			Ba-131	1,15E+01	1,56E+03
Ce-139	1,38E+02	2,14E+04	Ce-139	1,38E+02	1,77E+03
Pm-143	2,65E+02	1,70E+04	Pm-143	2,65E+02	6,75E+02
Eu-146	4,59E+00	1,01E+06	Eu-146	4,59E+00	3,76E+03
			Gd-146	4,83E+01	5,15E+03
Eu-147	2,40E+01	8,02E+04	Eu-147	2,40E+01	2,95E+03
			Eu-148	5,45E+01	2,46E+02
Yb-169	3,20E+01	1,71E+05	Yb-169	3,20E+01	9,77E+03
Lu-171	8,24E+00	2,81E+04	Lu-171	8,24E+00	2,07E+03
Lu-172	6,83E+02	1,57E+04	Lu-172	6,83E+00	1,62E+03
Lu-173	5,00E+02	3,46E+04	Lu-173	5,00E+02	3,06E+03
Hf-175	7,00E+01	1,43E+05	Hf-175	7,00E+01	1,62E+04
Ta-182	1,14E+02	1,26E+04	Ta-182	1,14E+02	2,80E+03
Re-183	7,00E+01	2,05E+05			
			Re-184	3,80E+01	8,02E+02
Os-185	9,36E+01	1,78E+05	Os-185	9,36E+01	2,09E+03
Tl-202	1,22E+01	2,86E+05	Tl-202	1,22E+01	3,61E+03
Bi-205	1,53E+01	1,51E+05	Bi-205	1,53E+01	1,95E+03
			Bi-206	6,24E+00	4,30E+02

(Lu _{0,8} Y _{0,2}) ₂ SiO ₅ :Ce (1 at. %)		
Nuclide	Halflife, days	Activity, Bq/unit
Rb-83	8,62E+01	4,85E+01
Sr-85	6,48E+01	1,25E+02
Y-88	1,07E+02	3,55E+02
Eu-146	4,59	1,27E+02
Tm-158	9,31E+01	1,47E+02
Yb-169	3,20E+01	6,81E+02
Lu-171	8,24E+00	4,43E+02
Lu-172	6,70E+00	2,63E+02
Lu-173	5,00E+02	4,97E+02
Lu176(naturally present)	1,38E+13	1,39E+02

Y ₂ SiO ₅ :Ce (1 at. %)		
Nuclide	Halflife, days	Activity, Bq/unit
Rb-83	8,62E+01	7,67E+02
Rb-84	3,28E+01	3,57E+02
Sr-85	6,48E+01	8,50E+02
Y-88	1,07E+02	3,33E+03
Zr-88	8,34E+01	1,32E+02



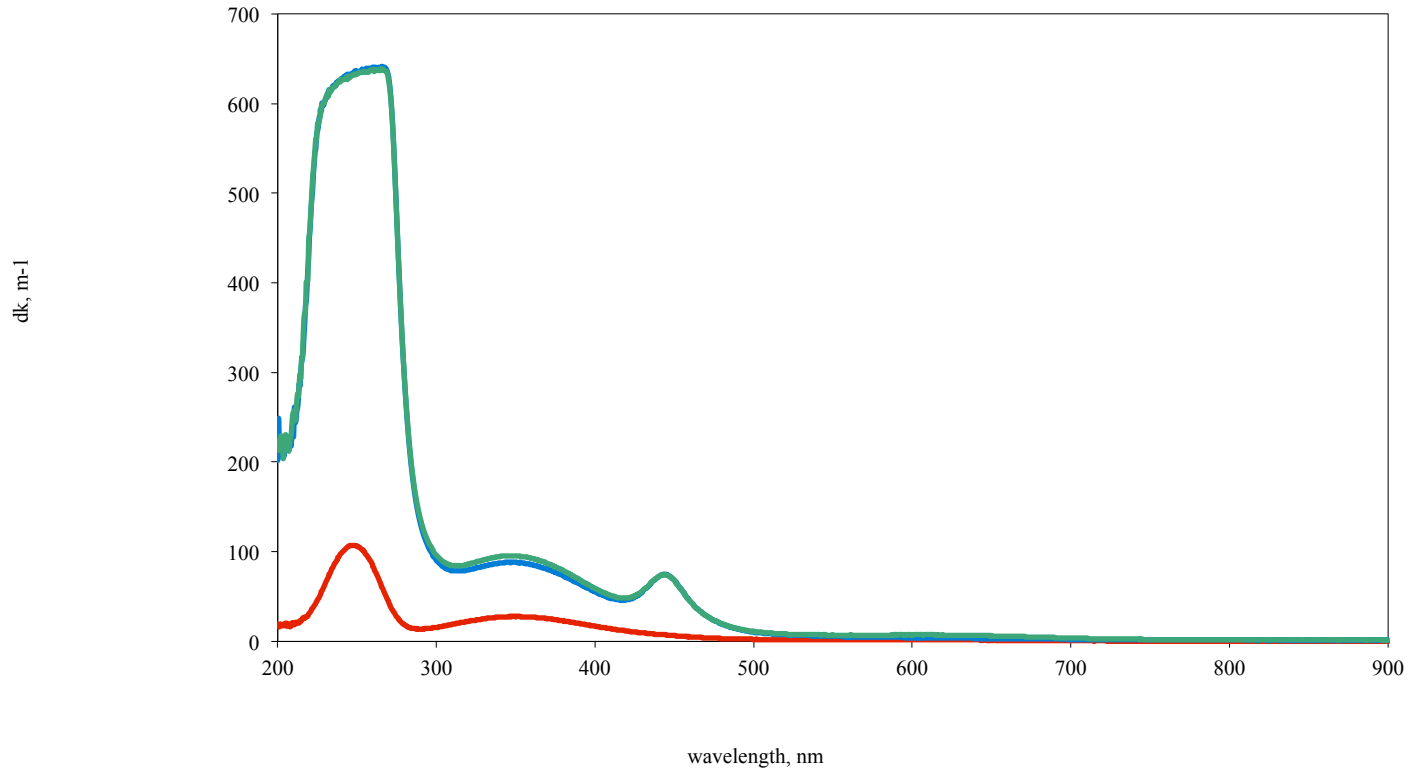
43.2 GeV/
(s·cm³)
from β+γ
emitters

6.4 GeV/(s·cm³)
from β+γ
emitters

Total energy,
deposited in
1cm³
by induced
radioisotopes

←
Set of the radio-isotopes generated in some inorganic scintillation crystals after irradiation with 24GeV protons with fluence $3 \cdot 10^{13}$ p/cm²

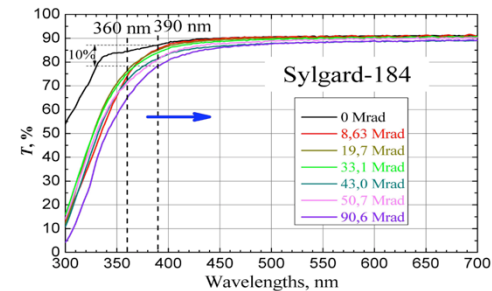
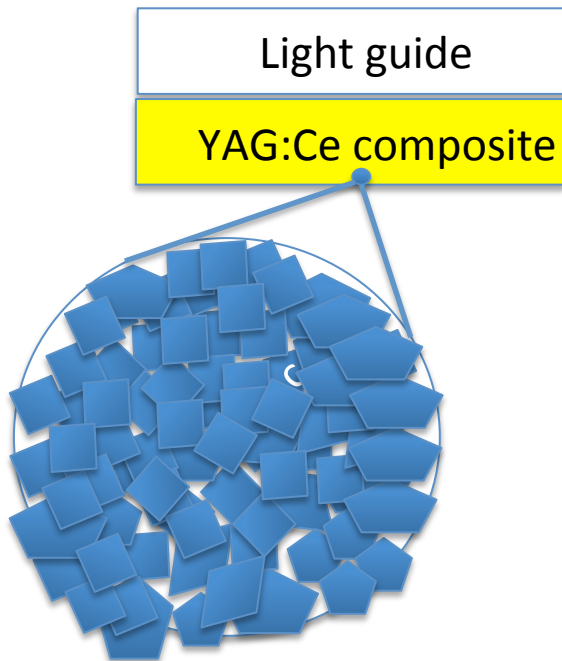
Lightweight of the material does not mean tolerance to radiation



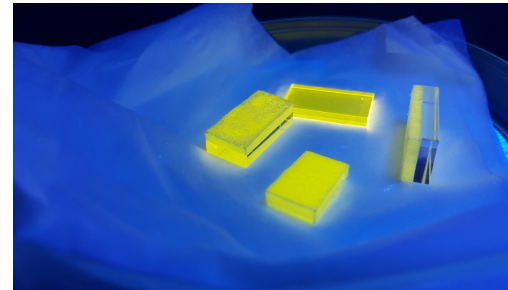
Comparison of induced absorption in LiF crystal after irradiation with 150MeV protons (green) and γ - irradiation (red)

From single crystals to composites

Key points- Proper choice of the dimensions of the grains;
Proper packing and gluing of particles.



Change of the 1mm thick polymerized glue transmission at Irradiation with gammas *Courtesy of A.Gektin and A.Boyarintsev)



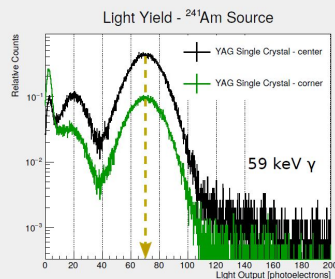
Illumination with 390nm light of YAG:Ce single crystal/quartz YAG:Ce composite/quartz

N29-12 Single Crystalline and Composite Scintillators for Hadron Calorimetry at High Luminosity LHC

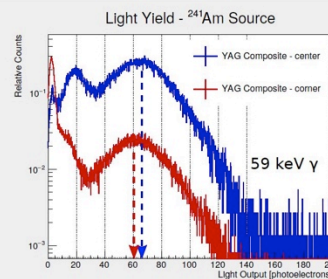
M. Lucchini¹, E. Auffray¹, A. Fedorov², J. Houžvicka³, M. Korzhik², D. Kozlov², V. Mechinsky², M. Nikl⁴, S. Ochesanu³

¹CERN, Switzerland; ²RINP, Belarus; ³CRYTUR, Czech Republic; ⁴Institute of Physics, Czech Republic

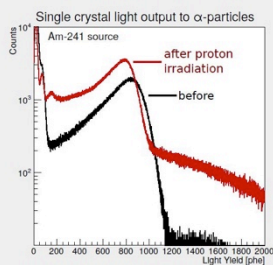
YAG:Ce scintillator versus YAG:Ce/quartz composite



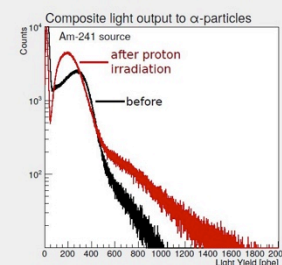
- ▶ Uniformity study performed using a ~ 3 mm thick Aluminum collimator to irradiate separately the center and corner of the scintillator volume.
- ▶ Single crystal show good uniformity of light output to 59 keV γ -rays from ^{241}Am source and variation of response is within $\sim 1\%$.



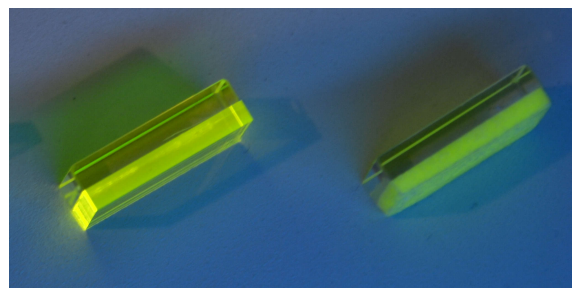
- ▶ Uniformity study performed using a ~ 3 mm thick Aluminum collimator to irradiate separately the center and the corner of the scintillator volume.
- ▶ Composite scintillator shows a small decrease of light output, **about 10%**, when excitation is close to the corner.



- ▶ **Irradiation with 24 GeV protons** performed at CERN PS to a fluence of $7 \times 10^{13} \text{ cm}^{-2}$. Both single crystal and composite were placed after a 15 cm PWO crystal to emulate effect of secondary particles due to absorber in real calorimeter.
- ▶ A drop of about 7% in light output is observed for single crystal and small increase in radioactivity of the sample (background).



- ▶ Before irradiation, **response of composite to alpha particles is smaller** than single crystal due to surface energy deposition combined with a strong bulk attenuation.
- ▶ After proton irradiation composite scintillator shows a drop of light output of about 30% most likely due to a darkening of the optical glue due to interactions of protons with light elements (H,C).

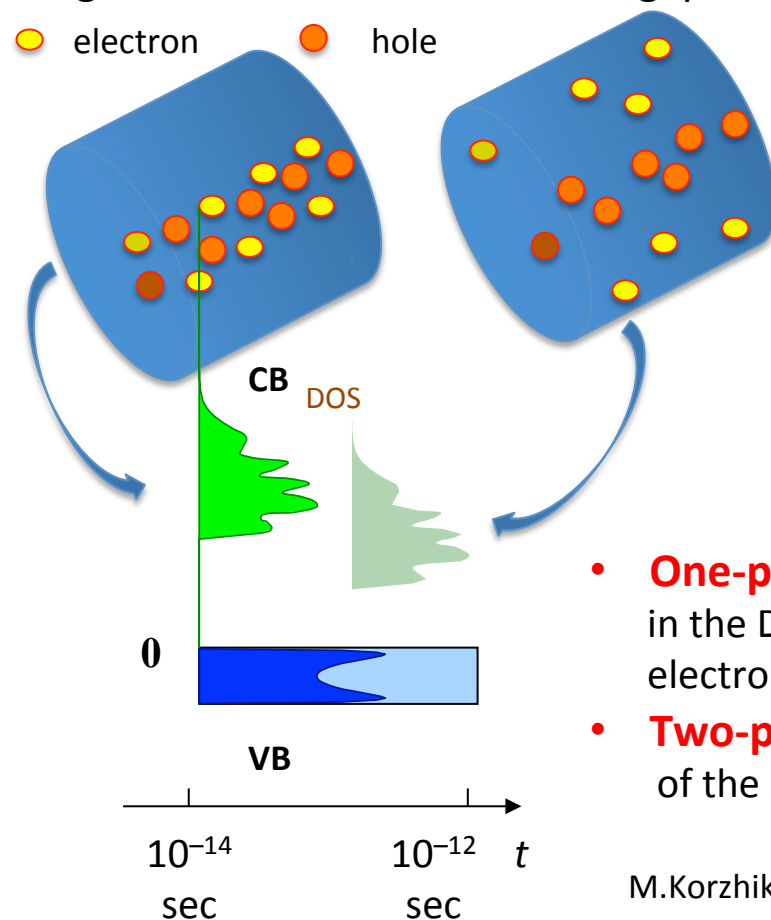


On the way to prevent damage of photo-sensors.

Two-photon absorption probing of the radiation excited media

Elastic polarization of the dielectric due to the local lattice distortion caused by the displacements of electrons and holes generated by the ionization.

Fragment of track of the ionizing particle



Spatial separation of holes and electrons leads to creation of electric field which distorts crystal lattice.

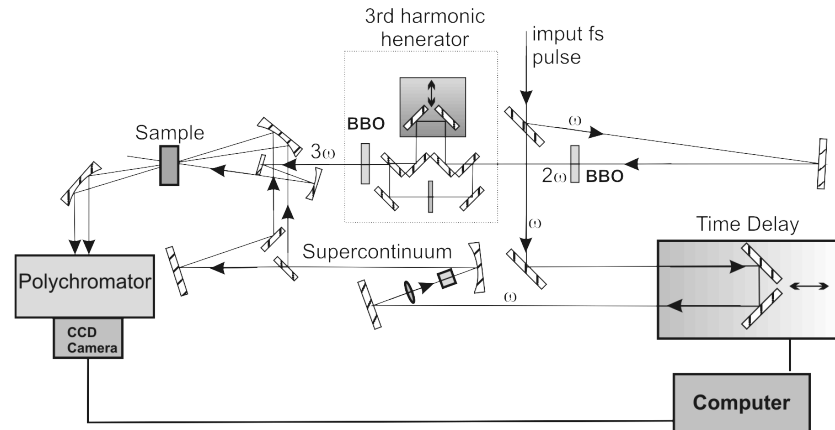
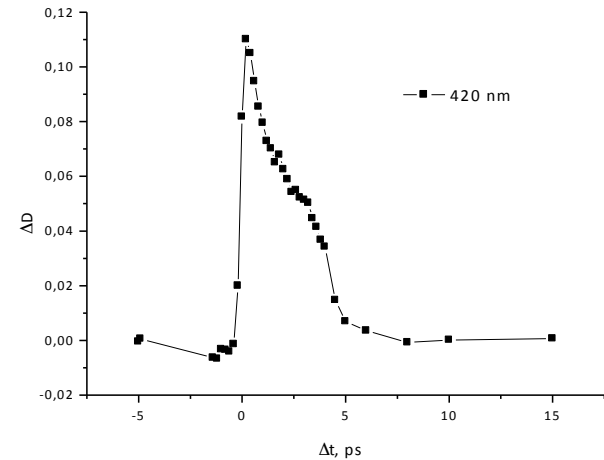
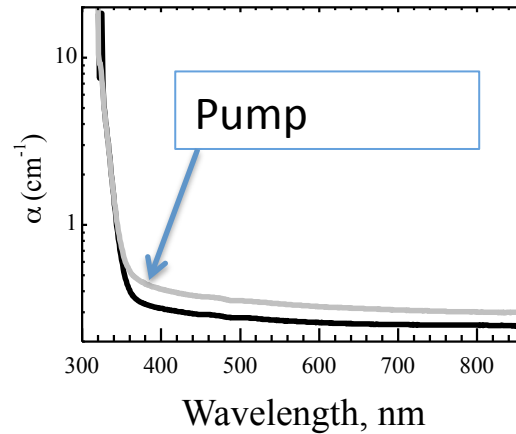
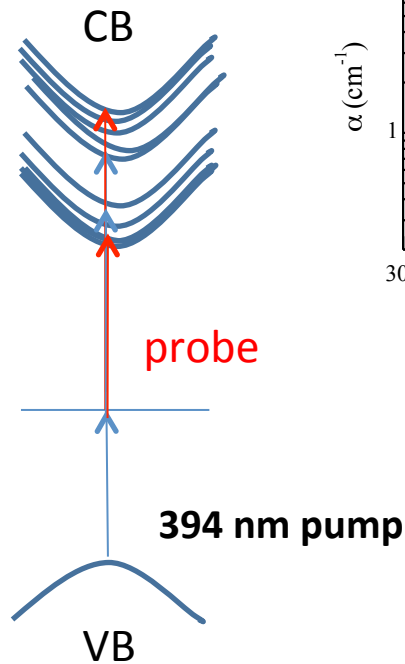
This local distortion in the lattice results in redistribution of the density of states (DOS) of electron in the conduction band in close vicinity of the hole.

The key feature of the elastic polarization: short response time

- **One-photon absorption** is not convenient to explore changes in the DOS due to strong absorption of single photons via electronic transitions between valence and conduction bands.
- **Two-photon absorption** becomes preferable due to change of the selection rules for interband transitions

Two-photon absorption in PWO

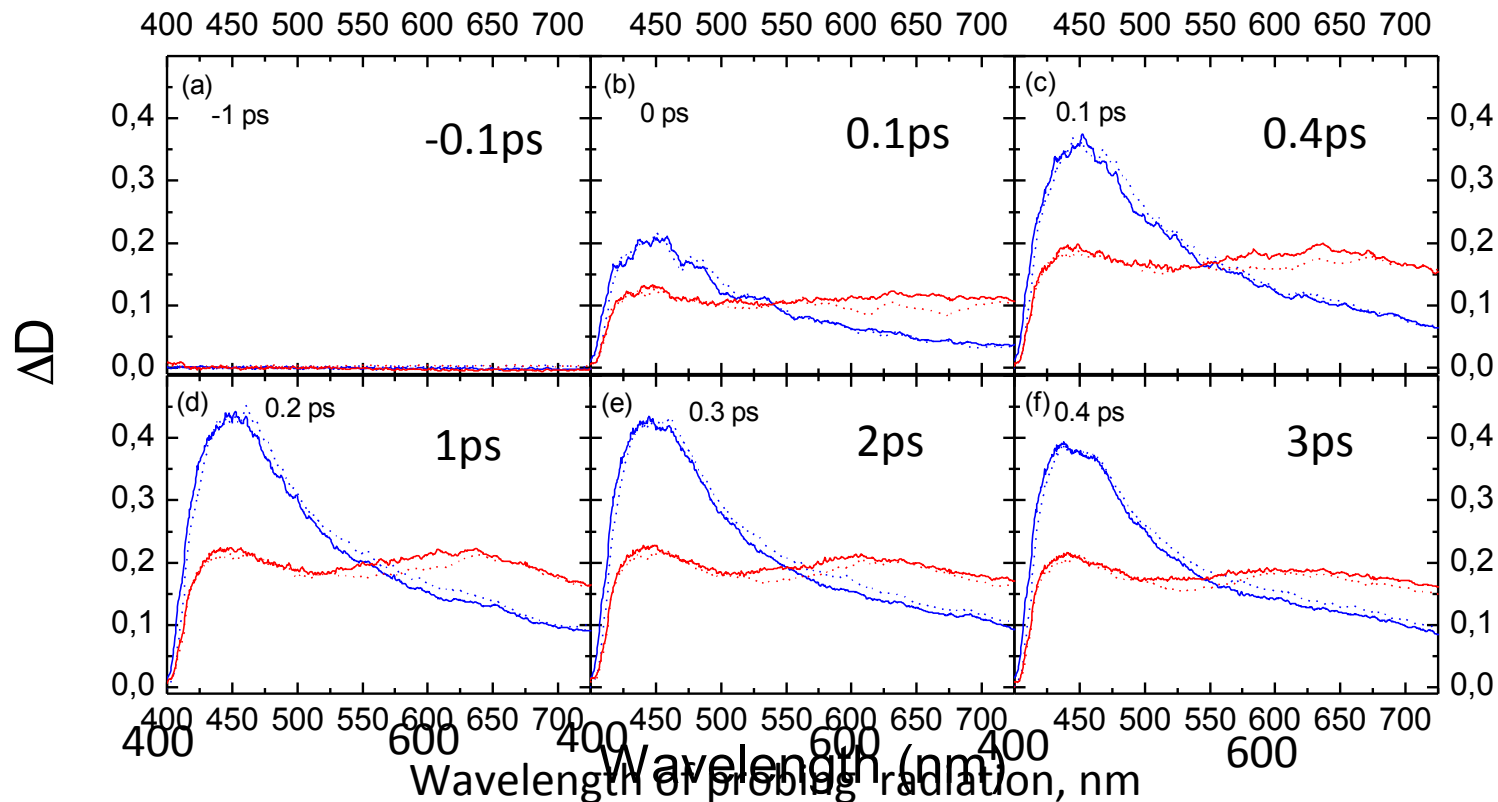
Two photon(2,97+3.16eV) absorption in 1 cm thick PWO .



E. Auffray, O.Buganov et al., New detecting techniques for future calorimetry, Journal of Physics: Conf. Series 587(2015) 012056

Experimental bench for 2 photon absorption measurements

Spectra of differential optical transmittance in PWO induced by 500 mJ/cm² pump at 395 nm

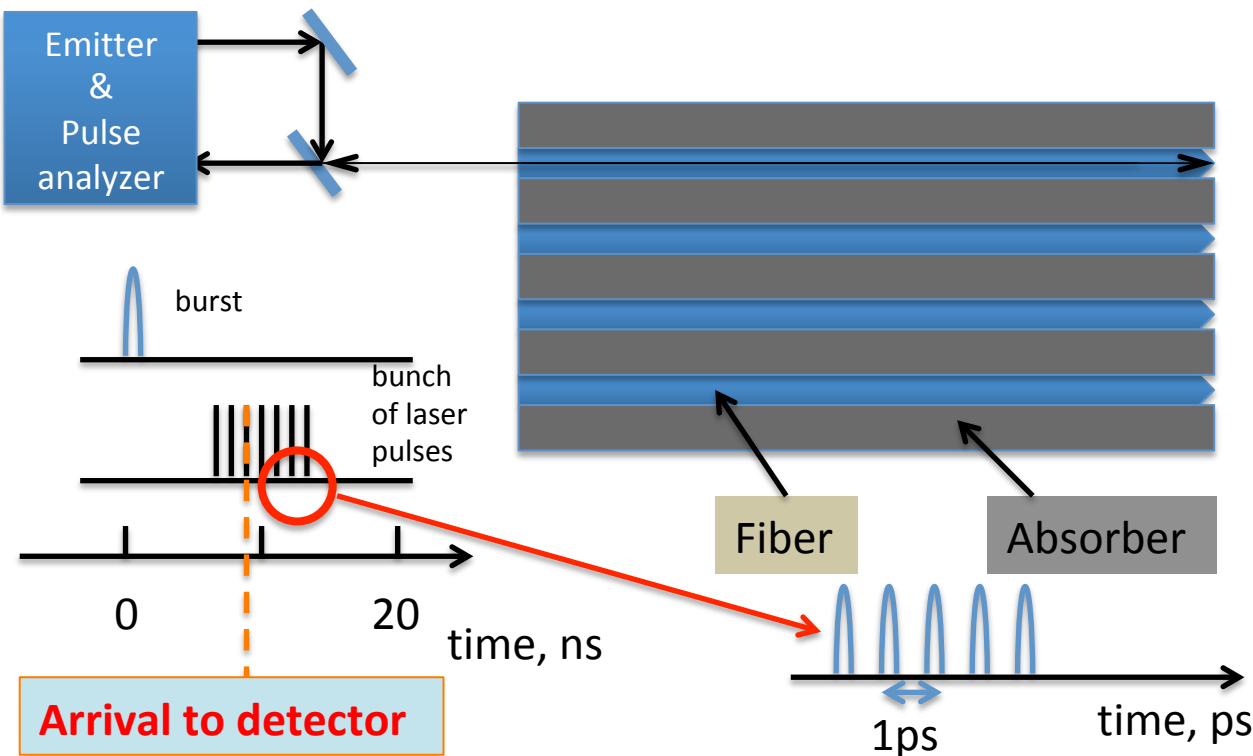


Pump polarized along the crystal axis **b** (blue lines) and polarized at 75° to the crystal axis **b** (red lines) under (dashed lines) and without (solid lines) gamma irradiation. Delays of probe pulse are indicated.

E. Auffray, O. Baganov, M. Korzhik, A. Fedorov, S. Nargelas, G. Tamulaitis, S. Tikhomirov, A. Vaitkevicius, [Application of two-photon absorption in PWO scintillator for fast timing of interaction with ionizing radiation](#), Nuclear Instruments and Methods in Physics Research Section A, 2015.

Sketch of the detecting module ,exploiting two-photon absorption

The second harmonic of their radiation can be used to produce the light in the wavelength range of 500-530 nm, which is optimal for PWO.

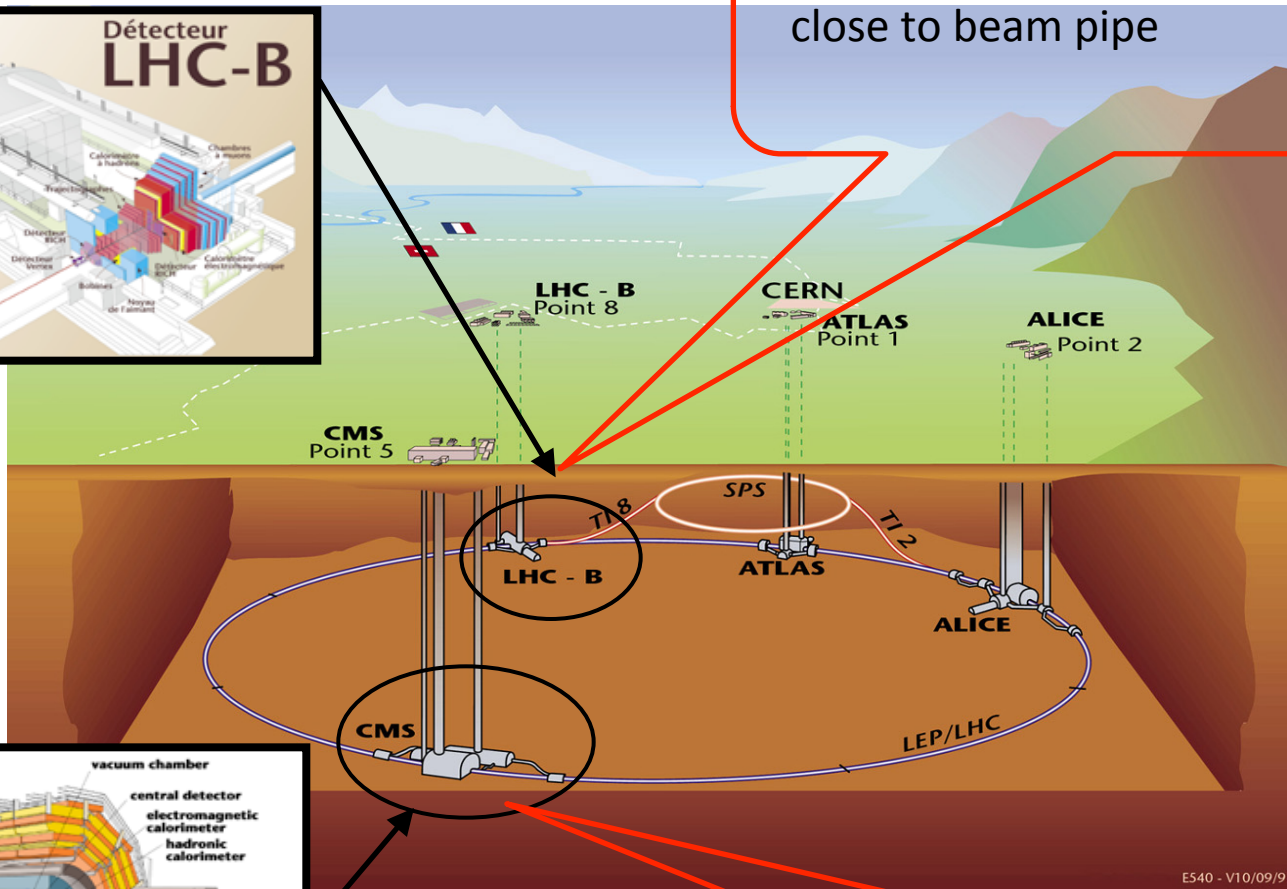
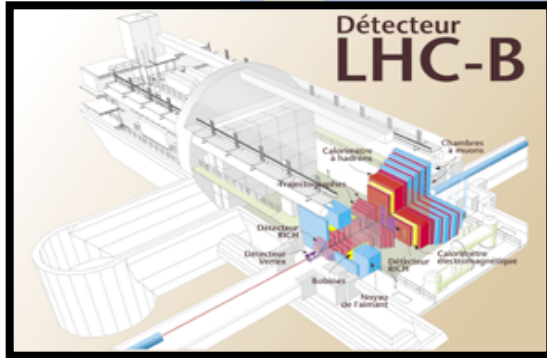


1. Fibers can have different refraction index to control light speed
2. Fibers can be also scintillating
3. Registration can be managed in a regime of standing or travelling wave

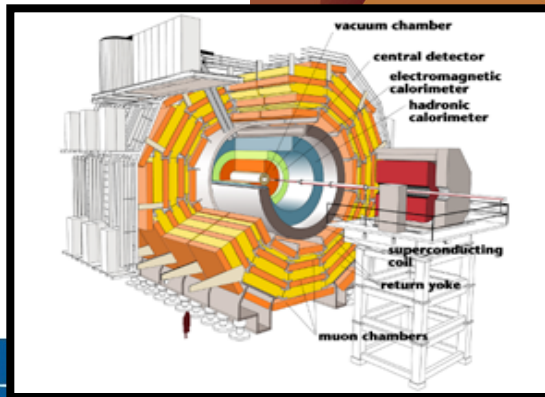
The light propagating along the scintillation crystal and reflected from the front face of the crystal could be used to observe the two-photon absorption.

LHC EXPERIMENTS

Replacement of the plastic scintillator by GAGG crystal in the part of the detector close to beam pipe



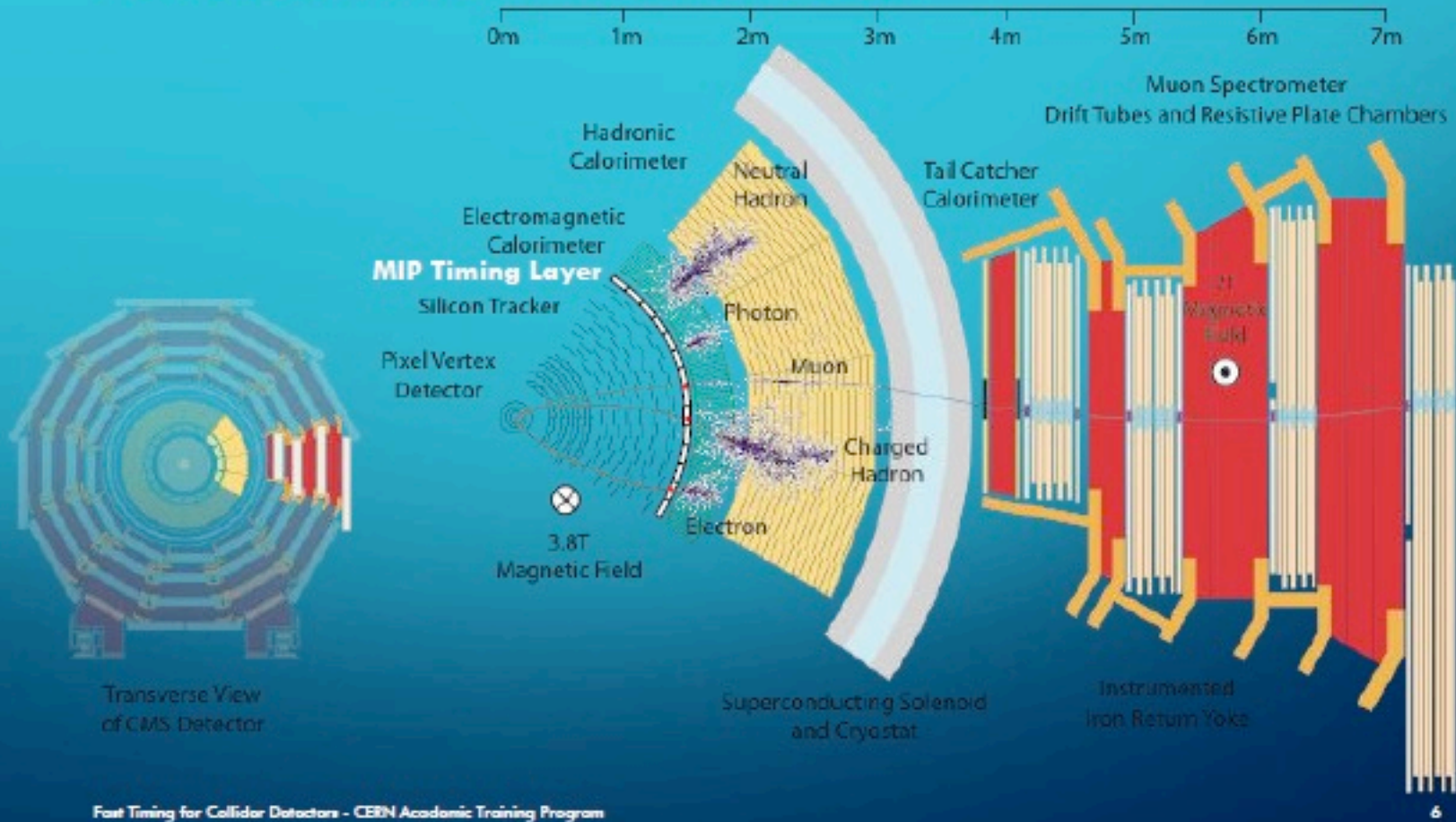
CMS



Incorporation in the detector of the thin crystal layer – Barrel Crystal Layer

Barrel time layer at CMS

Particle-flow Event Reconstruction



Courtesy of CMS BTL group

M.Korzhik, Grodno, APMP, 13.08.2018



CRYSTAL CLEAR COLLABORATION (RD18) at CERN: Scintillation materials development



Crystal 2000-1992

MR594 - San Francisco

SCINT95 - Delft

SCINT97 - Shanghai

SCINT99 - Moscow

SCINT2001 - Chamonix

SCINT2003 - Valencia

ISMART2004(JINR)

SCINT2005 - Alushta

SCINT2007 - Wake Forest

ISMART2008(Kharkov)

SCINT2009 - Jegu Island

ISMART2010(Kharkov)

SCINT2011 - Giessen

SCINT2013 - Shanghai

ISMART 2014 (Minsk)

SCINT2015 - Berkeley

ISMART 2016 (Minsk)

SCINT2017 - Chamonix

ISMART 2018

(Minsk)

Crystal Clear is a driving force of the "SCINT" Conference Series since beginning

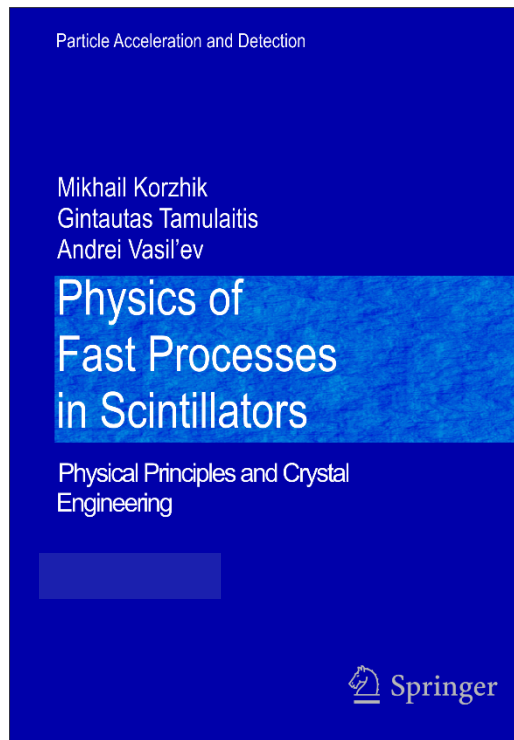


Research group from INP BSU is active for 30 years in the scintillation materials development for detector systems

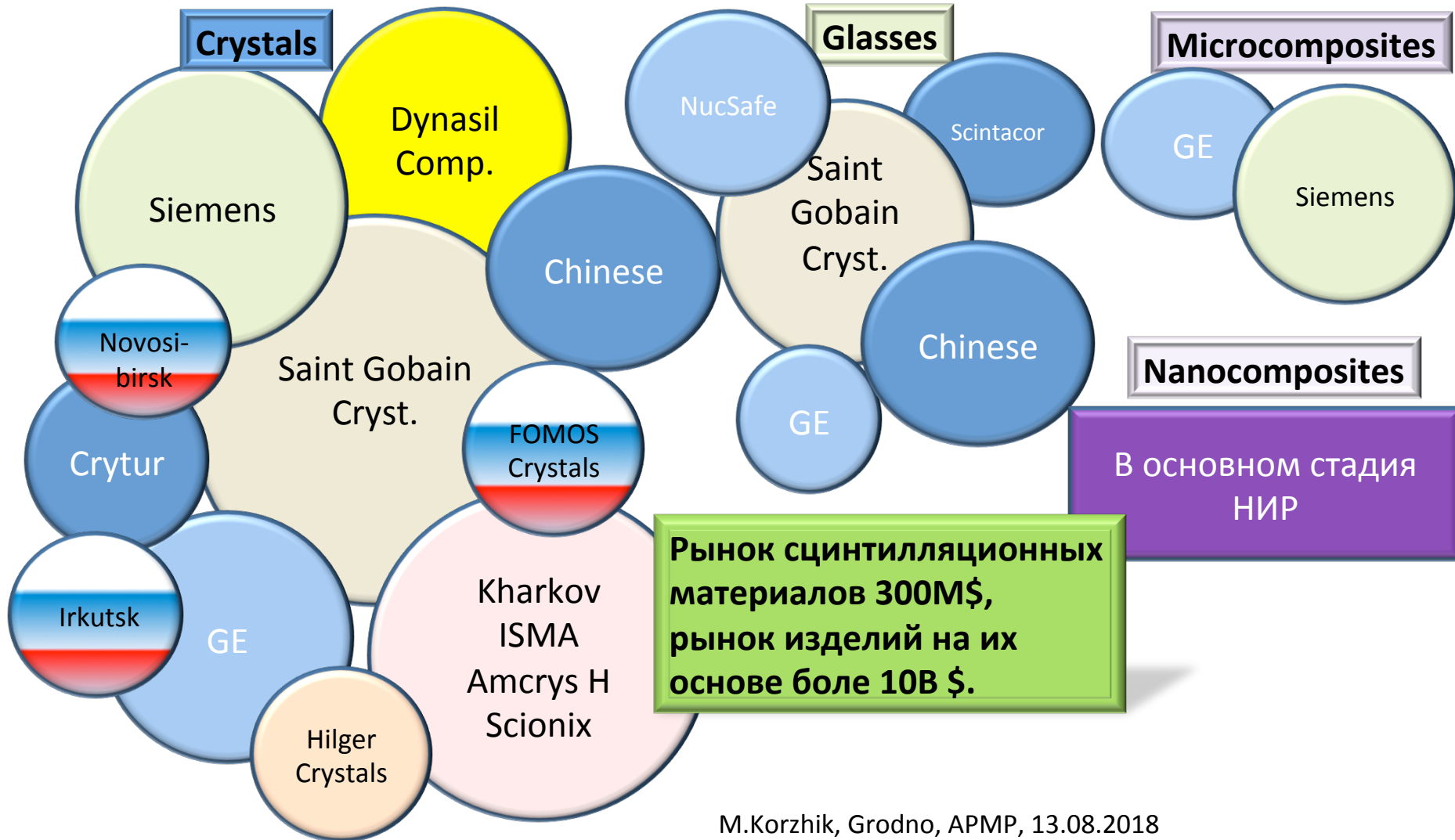
•



Coming soon!



Производство сцинтилляционных материалов. Состояние рынка и основные производители.



Acknowledgement

Author expresses gratitude to colleagues from CMS, Crystal Clear Collaboration at CERN and PANDA Collaboration at FAIR(GSI), especially, Dr. P.R.M.Lecoq, A.Fedorov, R.W. Novotny, H.G.Zaunick, K.Th. Brinkmann Dr. E.Auffrtay, Prof. G. Tamulaitis, for a long time joint research of the effects in inorganic scintillation materials, V.Dormenev, V.Mechinsky, M.Lucchini, for a productive joint research and fruitful discussions, A.Singovski, M.Glaser, A. Machard, V. Panov, R. Zoueusky, and A.Barysevich for assistance in the measurements.

The work is supported by grant № 14.W03.31.0004 of Russian Federation Government, BRFFI, State Scientific Program of Republic of Belarus “Convergence” , COST FAST ACTION MD1401, MSC RISE Intelum and AIDA 2 Horizon 2020 Projects .